SKI Report 02:37

Research

Theoretical and Numerical Evaluation of the MTC Noise Estimate in 2-D 2-group Heterogeneous Systems

Christophe Demazière

January 2002

ISSN 1104–1374
ISRN SKI-R-02/37-SE

SKI PERSPECTIVE

How this project has contributed to SKI's research goals

The overall goals for SKI research are:

- to give a basis for SKI 's supervision
- to maintain and develop the competence and research capacity within areas which are important to reactor safety
- to contribute directly to the Swedish safety work.

The project has contributed to the research goal of giving a basis for SKI's supervision by developing a non-intrusive method for determination of the moderator temperature coefficient (MTC) in pressurized water reactors (PWRs). The MTC is an important safety parameter which has to be measured twice during a fuel cycle in PWRs.

Furthermore, the project has also contributed to the strategical research goal of competence and research capacity by building up competence within the Department of Reactor Physics at Chalmers University of Technology regarding reactor physics, reactor dynamics and noise diagnostics.

Project information:

Project manager:	Ninos Garis, Department of Reactor Technology, SKI
Project number:	14.5-011142-01261
Previous reports:	SKI report 00:28 (2000).

SKI Report 02:37

Research

Theoretical and Numerical Evaluation of the MTC Noise Estimate in 2-D 2-group Heterogeneous Systems

Christophe Demazière

Chalmers University of Technology
Department of Reactor Pysics
412 96 Göteborg
Sweden

January 2002

This report concerns a study which has been conducted for the Swedish Nuclear Power Inspectorate (SKI). The conclusions and viewpoints presented in the report are those of the author/authors and do not necessarily coincide with those of the SKI.

SKI Project Number 01261

Table of contents

Summary/Sammanfattning **5**

1. Introduction **6**

2. Calculation of the static flux, the adjoint flux, and the reactor transfer function **7**

2.1. Description of the core 8

2.2. Description of the static core simulator 11

2.3. Description of the adjoint core simulator 17

2.4. Description of the noise simulator 19

3. Derivation of the MTC noise estimators for 2-D 2-group heterogeneous systems **25**

3.1. Calculation of the reactivity noise in multigroup perturbation theory 25

3.2. Calibration of the noise simulator results to the SIMULATE-3 results 32

3.3. Derivation of the MTC noise estimators in the 2-D 2-group approximation 32

4. Results **38**

4.1. Specification of the noise source 38

4.2. Calculated MTC noise estimators 39

5. Conclusions **43**

6. References **44**

7. Nomenclature **45**

Summary

The effect of a heterogeneous distribution of the temperature noise on the MTC estimation by noise analysis is investigated. This investigation relies on the 2-group diffusion theory, and all the calculations are performed in a 2-D realistic heterogeneous core. It is shown, similarly to the 1-D case, that the main reason of the MTC underestimation by noise analysis compared to its design-predicted value lies with the fact that the temperature noise might not be homogeneous in the core, and therefore using the local temperature noise in the MTC noise estimation gives erroneous results. A new MTC estimator, which was previously proposed for 1-D 1-group homogeneous cases and which is able to take this heterogeneity into account, was extended to 2-D 2-group heterogeneous cases. It was proven that this new estimator is always able to give a correct MTC estimation with an accuracy of 4%. This small discrepancy comes from the fact that the reactor does not behave in a point-kinetic way, contrary to the assumptions used in the noise estimators. This discrepancy is however quite small.

One quantitative result of the present work is a measure of the underestimation of the traditional method as a function of the correlation length of the temperature fluctuations. It is found that the underestimation is larger in 2-D for the same correlation length as in the 1-D case. An underestimation with a factor 5 in the present model is obtained with a radial correlation length of 150 cm. Comparisons with measurements will be possible to make in measurements to be performed in Ringhals.

Sammanfattning

Inverkan av den inhomogena rumsfördelningen av temperaturfluktuationerna för bestämningen av MTK (moderatortemperaturkoefficienten) med brusanalys har undersökts och rapporterats. Undersökningen i detta arbete är baserad på tvågruppsdiffusionsteori. Alla beräkningar har gjorts i en 2-D realistisk reaktorhärd. Liksom i en tidigare undersökning i 1-D finner vi, att den huvudsakliga anledningen till att den traditionella brusmetoden underskattar moderatortemperturkoefficienten är inhomogeniteten av temperaturfluktuationerna, varför användning av ett lokalt värde på temperaturfluktuationerna ger felaktigt resultat. Den nya så kallade estimatorn, det vill säga en algoritm för bestämning av MTK, som nyligen har föreslagits och testats av oss i 1-D, har nu utvidgats till att omfatta 2-D 2-gruppsteorin. Undersökningarna som rapporteras här visar, att den nya estimatorn skattar den verkliga temperaturkoefficienten med en noggrannhet på 4 %. Det jämförelsevis lilla felet härrör från reaktorresponsens avvikelse från punktkinetik, eftersom även den nya algoritmen förutsätter att reaktorns beteende är punktkinetiskt. Denna avvikelse är dock ganska liten.

Ett resultat av föreliggande arbete är det kvantitativa sambandet mellan underskattning av MTK med den traditionella brusmetoden och korrelationslängden av temperaturfluktuationerna. Vi fann att underskattningen i 2-D vid en viss korrelationslängd är större än i 1-D. En underskattning med en faktor 5 erhålls i föreliggande arbete vid en korrelationslängd på 150 cm. Jämförelse med mätningar från Ringhals kommer att göras.

1. Introduction

There have been many attempts in the past few years to monitor the Moderator Temperature Coefficient of reactivity (MTC) by noise analysis in Pressurized Water Reactors (PWRs). In these experimental investigations, the MTC is inferred from the signals delivered by an in-core neutron detector and a core-exit thermocouple located in the same fuel channel or in two neighbouring fuel channels. The measured neutron noise and temperature noise contain some information about the dynamics of the reactor, and in particular on the MTC, while the reactor is still at its normal and steady-state operating conditions. This noise technique is therefore very well suited to monitor the MTC at full power, since unlike the traditional measurement techniques such as the boron dilution method or the control rod swap, the reactor does not need to be perturbed.

Due to the reactor transient that the traditional measurement techniques induce and their relatively large uncertainty on the MTC estimation, it was considered that measuring the at-power MTC could be avoided, since core calculations were believed to give an accurate estimation of the at-power MTC. Thus a more and more common practice was to measure the MTC at Beginning of Cycle (BOC) and Hot Zero Power (HZP), a measurement which is accurate and relatively easy to perform, and then to rely completely on core calculations for the variation of the MTC with burnup. Nevertheless, this at-power MTC calculation was never benchmarked. Furthermore, with the use of high burnup or Mixed Oxide (MOX) fuel assemblies, the MTC might become positive at BOC. For the high burnup fuel bundles, the positive contribution is due to the high boron concentration necessary to compensate for the reactivity excess of the fuel. For the MOX fuel, the positive contribution is due to the 0.3 eV resonance of Pu-239. Therefore being able to monitor the MTC throughout the whole fuel cycle could become again of great interest in the near future. The noise technique is very interesting in this respect, since such a measurement can be carried out at any time during the fuel cycle without disturbing the reactor operation.

Nevertheless, all the experimental work revealed that the MTC was systematically underestimated by a factor of two to five compared to its design-predicted value (see (Demazière, 2000) for a complete list of References in this matter). This underestimation was found to be constant during a fuel cycle, and even between several fuel cycles as long as the same pair of detectors is used for the estimation. Many factors could influence the accuracy of the MTC noise estimation. Several of them were investigated in the past. Although correction factors were proposed accordingly, either the correction factors are negligible, or they cannot be estimated easily in practice. A new aspect which could explain the underestimation of the noise analysis technique was considered recently (Pázsit et al, 2000), (Demazière and Pázsit, 2002), namely the spatially heterogeneous distribution of the temperature noise throughout the core. It was found that the main reason of the MTC underestimation might be due to the fact that the temperature noise was measured in one-point of the reactor, whereas the MTC relies on the core average temperature noise and that this temperature noise is most likely strongly spatially heterogeneous. The spatial inhomogeneity of the temperature noise has actually been confirmed in recent measurements (Demazière et al, 2000a). On the other hand, the resulting deviation of the reactor response from point-kinetics, an approximation on which the MTC noise estimator relies, was found to be negligible with respect to the

MTC estimation. Consequently, one new MTC noise estimator that allows taking the spatial structure of the temperature noise into account was proposed by us recently and was proven to give an accurate MTC estimation (Pázsit et al, 2000), (Demazière and Pázsit, 2002).

This above mentioned study only investigated 1-D one-group homogeneous systems in the diffusion approximation. In this report, the investigation is extended to 2-D two-group heterogeneous systems in the diffusion approximation. The main goals of the work were as follows:

1. To extend the definition of the average temperature to a 2-group case (this is not trivial); with the definition, give a new biased estimator for the determination of the MTC which is only biased with the deviation of the reactor response from point kinetics;
2. To elaborate calculational methods for the investigation of the performance of the traditional and the new estimators in 2-D 2-group theory;
3. To verify that the qualitative conclusions of the 1-D investigation regarding the reason of the underestimation of the MTC by the traditional method are similar in 2-D;
4. To investigate quantitatively the dependence of the magnitude of the MTC underestimation by the traditional noise method as a function of the correlation length of the temperature fluctuations.

The first part of the report is devoted to the models used in the simulation. The second part deals with the derivation of the MTC noise estimate for 2-D 2-group heterogeneous systems, which is slightly different from the 1-D 1-group homogeneous systems. Finally, the results of the calculations are presented in more detail. It was found that the new MTC estimator was always able to give a correct MTC estimation. This finding further confirms that the deviation of the reactor response from point-kinetics does not play a significant role for the MTC estimation, whereas the spatial inhomogeneity of the temperature noise has a very decisive effect. The usual MTC noise estimator was found to underestimate the MTC more significantly than for the 1-D one-group homogeneous cases.

A nomenclature explaining all the abbreviations used in this report can be found at the end (see Section 7).

2. Calculation of the static flux, the adjoint flux, and the reactor transfer function

The traditional MTC noise estimator, i.e. the one that was used in all the experimental work so far, is based on the measurement of the temperature noise, the induced neutron noise, and the static flux. As will be described in more detail in Section 3, the new MTC noise estimator in addition relies also on the adjoint flux, which is needed for the calculation of the core average temperature noise. Consequently, a static core simulator, an adjoint core simulator, and a noise simulator are required for the theoretical investigation of the MTC estimation by noise analysis.

2.1. Description of the core

A realistic heterogeneous system was chosen for this investigation, namely the Ringhals-4 PWR with the operational conditions as of May 5th, 1999. At that date, the at-power MTC was measured by using the boron dilution method. This measurement was performed a few months before the expected EOC of the fuel cycle 16, more precisely at a core average burnup of 8.767 GWd/tHM. This measurement, which is required by the Swedish safety authorities, is intended to verify that the magnitude of the MTC will not exceed a given value for the remaining part of the cycle, therefore preventing from the consequences of a reactivity transient, induced by an incidental cooldown event. During this measurement, the MTC was found to be equal to -58.12 pcm/°C ± 11.68 pcm/°C (Demazière et al, 2000b). The MTC was also directly calculated by SIMULATE-3 (Umbarger and DiGiovine, 1992) by simply increasing the coolant inlet temperature by +5 °F (2.78 °C), all the other parameters remaining constant. It was found that:

$$MTC = -45.882 \text{ pcm/°C} \tag{1}$$

This value will be considered in the following as the reference and target value[1] of the MTC for the noise analysis technique.

As will be seen in the following, the 2-D 2-group material data and the point-kinetic parameters of the core are required for the calculation of the induced neutron noise via the noise simulator. Furthermore, the static flux and the adjoint flux are also required in this 2-D and 2-group derivation. The static flux is needed for the neutron noise simulator itself and the MTC estimation in the noise analysis technique, whereas the adjoint flux is used (together with the static flux) for calculating the core average temperature noise. One could use SIMULATE-3 to provide all these quantities. Nevertheless, the static and adjoint fluxes need to be recalculated via a simulator using the same spatial discretisation scheme as the one used in the neutron noise simulator. Otherwise, using the static and adjoint fluxes directly from SIMULATE-3 is equivalent to make the system non-critical[2]. Another simpler approach could have been to modify the cross-sections in each node (while keeping the static and adjoint fluxes from SIMULATE-3) so that the balance equations were fulfilled for the same spatial discretisation scheme as the one used in the noise simulator. This approach was tested in the present case but showed that some cross-sections became negative.

Hence, the 2-group cross-sections provided by SIMULATE-3 for each node were homogenised from 3-D to 2-D in order to be used by the 2-D simulators. The homogenization was naturally carried out by using the static fluxes as weighting functions so that the reaction rates were preserved:

---

1. Only the ratios between the MTC noise estimators and the actual value of the MTC are investigated in this study. The MTC is only evaluated in relative terms, therefore the actual MTC value does not really matter since the MTC noise estimators can be scaled to any value (see Section 3.2).
2. The static and adjoint fluxes (and their associated eigenvalues) are nevertheless used in the static and adjoint core simulators as a starting guess in the power iteration method.

$$XS_{G,I,J} = \frac{\sum_K XS_{G,I,J,K}\phi_{G,I,J,K}V_{I,J,K}}{\sum_K \phi_{G,I,J,K}V_{I,J,K}} \tag{2}$$

and

$$\phi_{G,I,J} = \frac{\sum_K \phi_{G,I,J,K}V_{I,J,K}}{\sum_K V_{I,J,K}} \tag{3}$$

with XS_G having a broad meaning, i.e. being D_G, $\Sigma_{a,G}$, Σ_{rem}, or $\nu\Sigma_{f,G}$. All the other symbols have their usual meaning with $V_{I,J,K}$ representing the volume of the node *(I,J,K)*. G is the group index ($G = 1$ for the fast group, and $G = 2$ for the thermal group). Similarly, the adjoint fluxes were homogenised as follows:

$$\phi^+_{G,I,J} = \frac{\sum_K \phi^+_{G,I,J,K}V_{I,J,K}}{\sum_K V_{I,J,K}} \tag{4}$$

Although this way of averaging the material data and the fluxes preserves the reaction rates, the 2-D system which is thus obtained will have a much higher eigenvalue than the 3-D system since the leakage in the axial direction was eliminated (a 2-D system is in fact assumed to be infinite in the third direction). Therefore, if one wants results compatible with the actual 3-D core, one has to take the axial leakage into account in the 2-D system. This can be done by increasing the absorption cross-section in each group by an artificial leakage cross-section in the same group, which allows having the correct leakage rate when multiplied by the corresponding group flux. For that purpose, one needs to evaluate the axial leakage rate in each node for the 3-D system. Since this leakage rate is not given by SIMULATE-3, the finite difference scheme is used instead (this finite difference scheme is also used in the static core simulator, the adjoint core simulator, and the neutron noise simulator). In the "box-scheme" approximation, this reads as (Nakamura, 1977):

$$\begin{aligned} &\text{leakage rate in group } G \text{ and node}(I,J,K) \\ &= -\frac{1}{\Delta z}[a^z_{G,I,J,K}\phi_{G,I,J,K} + b^z_{G,I,J,K}\phi_{G,I,J,K+1} + c^z_{G,I,J,K}\phi_{G,I,J,K-1}] \\ &= LR_{G,I,J,K} \end{aligned} \tag{5}$$

with the coefficients $a^z_{G,I,J,K}$, $b^z_{G,I,J,K}$, and $c^z_{G,I,J,K}$ given by the following Table 1:

Table 1: Coupling coefficients in the z direction.

	$a^z_{G,I,J,K}$	$b^z_{G,I,J,K}$	$c^z_{G,I,J,K}$
if the node *K-1* does not exist	$\frac{2D_{G,I,J,K}D_{G,I,J,K+1}}{\Delta z(D_{G,I,J,K}+D_{G,I,J,K+1})} + \frac{2D_{G,I,J,K}}{\Delta z}$	$-\frac{2D_{G,I,J,K}D_{G,I,J,K+1}}{\Delta z(D_{G,I,J,K}+D_{G,I,J,K+1})}$	0
if the nodes *K-1* and *K+1* both exist	$\frac{2D_{G,I,J,K}D_{G,I,J,K+1}}{\Delta z(D_{G,I,J,K}+D_{G,I,J,K+1})} + \frac{2D_{G,I,J}D_{G,I,J,K-1}}{\Delta z(D_{G,I,J,K}+D_{G,I,J,K-1})}$	$-\frac{2D_{G,I,J,K}D_{G,I,J,K+1}}{\Delta z(D_{G,I,J,K}+D_{G,I,J,K+1})}$	$-\frac{2D_{G,I,J,K}D_{G,I,J,K-1}}{\Delta z(D_{G,I,J,K}+D_{G,I,J,K-1})}$
if the node *K+1* does not exist	$\frac{2D_{G,I,J,K}}{\Delta z} + \frac{2D_{G,I,J,K}D_{G,I,J,K-1}}{\Delta z(D_{G,I,J,K}+D_{G,I,J,K-1})}$	0	$-\frac{2D_{G,I,J,K}D_{G,I,J,K-1}}{\Delta z(D_{G,I,J,K}+D_{G,I,J,K-1})}$

The corresponding "leakage" cross-sections are thus given by:

$$L_{G,I,J,K} = -\frac{LR_{G,I,J,K}}{\phi_{G,I,J,K}} \tag{6}$$

so that the absorption cross-sections are modified in the following way:

$$\Sigma^*_{a,G,I,J,K} = \Sigma_{a,G,I,J,K} + L_{G,I,J,K} \tag{7}$$

Then the homogenization is carried out as described before, i.e. according to Eq. (2).

Concerning the noise calculation described in Section 2.4, one has to select also the frequency at which the evaluation has to be performed. In the MTC investigation by noise analysis, it is common practice to determine the MTC in the frequency range 0.1 - 1.0 Hz. The lower frequency bound allows using in the MTC noise estimators the zero-power reactor transfer function instead of the at-power reactor transfer function (which is unknown since it contains the MTC). This substitution is valid because the cut-off frequency corresponding to the heat transfer between coolant and fuel is lower than 0.1 Hz. The upper bound is due to the damping of the temperature fluctuations travelling from the in-core neutron detector to the core-exit thermocouple, if the traditional noise

estimator is used. In our case, the axial direction is disregarded, so that the upper limit has no significance. It was therefore decided to perform all the noise calculations at that frequency, i.e. 1 Hz.

2.2. Description of the static core simulator

As described previously, the static flux is needed in this theoretical investigation for three main reasons. First of all, the static flux is required for the calculation of the neutron noise, since the noise source strength is always proportional to the static flux (see Section 2.4). Second, the static flux is used in the MTC noise estimators, since only the neutron noise relative to its mean value is of interest (see Section 3). Finally, the static flux is used together with the adjoint flux to calculate the coolant average temperature noise throughout the core (see Section 3).

In the two-group diffusion approximation, the static flux is the solution of the following matrix equation:

$$[\bar{\bar{D}}(\boldsymbol{r})\nabla^2 + \bar{\bar{\Sigma}}(\boldsymbol{r})] \times \begin{bmatrix} \phi_1(\boldsymbol{r}) \\ \phi_2(\boldsymbol{r}) \end{bmatrix} = 0 \tag{8}$$

where

$$\bar{\bar{D}}(\boldsymbol{r}) = \begin{bmatrix} D_1(\boldsymbol{r}) & 0 \\ 0 & D_2(\boldsymbol{r}) \end{bmatrix} \tag{9}$$

$$\bar{\bar{\Sigma}}(\boldsymbol{r}) = \begin{bmatrix} \dfrac{\nu\Sigma_{f,1}(\boldsymbol{r})}{k_{eff}} - \Sigma_{a,1}(\boldsymbol{r}) - \Sigma_{rem}(\boldsymbol{r}) & \dfrac{\nu\Sigma_{f,2}(\boldsymbol{r})}{k_{eff}} \\ \Sigma_{rem}(\boldsymbol{r}) & -\Sigma_{a,2}(\boldsymbol{r}) \end{bmatrix} \tag{10}$$

This system of equations has to be spatially discretised. Finite differences were used for that task, and more precisely the so-called "box-scheme" (more information regarding this specific point can be found in (Pázsit et al, 2000) and (Pázsit et al, 2001), where the discretisation scheme was extensively explained):

$$\begin{aligned} &\frac{1}{\Delta x \cdot \Delta y} \int_{(I,J)} D_G(\boldsymbol{r})\nabla^2\phi_G(\boldsymbol{r})d\boldsymbol{r} \\ &= -\frac{(a^x_{G,I,J}\phi_{G,I,J} + b^x_{G,I,J}\phi_{G,I+1,J} + c^x_{G,I,J}\phi_{G,I-1,J})}{\Delta x} \\ &- \frac{(a^y_{G,I,J}\phi_{G,I,J} + b^y_{G,I,J}\phi_{G,I,J+1} + c^y_{G,I,J}\phi_{G,I,J-1})}{\Delta y} \end{aligned} \tag{11}$$

with the different coefficients $a^x_{G,I,J}$, $a^y_{G,I,J}$, $b^x_{G,I,J}$, $b^y_{G,I,J}$, $c^x_{G,I,J}$, and $c^y_{G,I,J}$ summarised in Table 2 and Table 3 for the *x* and *y* directions respectively.

Table 2: Coupling coefficients in the x direction.

	$a^x_{G,I,J,K}$	$b^x_{G,I,J,K}$	$c^x_{G,I,J,K}$
if the node *I-1* does not exist	$\frac{2D_{G,I,J}D_{G,I+1,J}}{\Delta x(D_{G,I,J}+D_{G,I+1,J})} + \frac{2D_{G,I,J}}{\Delta x}$	$-\frac{2D_{G,I,J}D_{G,I+1,J}}{\Delta x(D_{G,I,J}+D_{G,I+1,J})}$	0
if the nodes *I-1* and *I+1* both exist	$\frac{2D_{G,I,J}D_{G,I+1,J}}{\Delta x(D_{G,I,J}+D_{G,I+1,J})} + \frac{2D_{G,I,J}D_{G,I-1,J}}{\Delta x(D_{G,I,J}+D_{G,I-1,J})}$	$-\frac{2D_{G,I,J}D_{G,I+1,J}}{\Delta x(D_{G,I,J}+D_{G,I+1,J})}$	$-\frac{2D_{G,I,J}D_{G,I-1,J}}{\Delta x(D_{G,I,J}+D_{G,I-1,J})}$
if the node *I+1* does not exist	$\frac{2D_{G,I,J}}{\Delta x} + \frac{2D_{G,I,J}D_{G,I-1,J}}{\Delta x(D_{G,I,J}+D_{G,I-1,J})}$	0	$-\frac{2D_{G,I,J}D_{G,I-1,J}}{\Delta x(D_{G,I,J}+D_{G,I-1,J})}$

Table 3: Coupling coefficients in the y direction.

	$a^y_{G,I,J,K}$	$b^y_{G,I,J,K}$	$c^y_{G,I,J,K}$
if the node *J-1* does not exist	$\frac{2D_{G,I,J}D_{G,I,J+1}}{\Delta y(D_{G,I,J}+D_{G,I,J+1})} + \frac{2D_{G,I,J}}{\Delta y}$	$-\frac{2D_{G,I,J}D_{G,I,J+1}}{\Delta y(D_{G,I,J}+D_{G,I,J+1})}$	0
if the nodes *J-1* and *J+1* both exist	$\frac{2D_{G,I,J}D_{G,I,J+1}}{\Delta y(D_{G,I,J}+D_{G,I,J+1})} + \frac{2D_{G,I,J}D_{G,I,J-1}}{\Delta y(D_{G,I,J}+D_{G,I,J-1})}$	$-\frac{2D_{G,I,J}D_{G,I,J+1}}{\Delta y(D_{G,I,J}+D_{G,I,J+1})}$	$-\frac{2D_{G,I,J}D_{G,I,J-1}}{\Delta y(D_{G,I,J}+D_{G,I,J-1})}$

Table 3: Coupling coefficients in the y direction.

	$a^y_{G,I,J,K}$	$b^y_{G,I,J,K}$	$c^y_{G,I,J,K}$
if the node *J+1* does not exist	$\frac{2D_{G,I,J}}{\Delta y} + \frac{2D_{G,I,J}D_{G,I,J-1}}{\Delta y(D_{G,I,J}+D_{G,I,J-1})}$	0	$-\frac{2D_{G,I,J}D_{G,I,J-1}}{\Delta y(D_{G,I,J}+D_{G,I,J-1})}$

The matrix equation given by Eq. (8) has to be used to determine both the two-group fluxes and the eigenvalue. This can be done via the so-called outer iteration that can be summarised as follows. If one rewrites Eqs. (8) - (10) as:

$$\overline{\overline{M}}(\boldsymbol{r}) \times \bar{\phi}(\boldsymbol{r}) = \frac{1}{k_{eff}} \overline{\overline{F}}(\boldsymbol{r}) \times \bar{\phi}(\boldsymbol{r}) \tag{12}$$

with

$$\overline{\overline{M}}(\boldsymbol{r}) = \begin{bmatrix} \Sigma_{a,1}(\boldsymbol{r}) + \Sigma_{rem}(\boldsymbol{r}) - D_1(\boldsymbol{r})\nabla^2 & 0 \\ -\Sigma_{rem}(\boldsymbol{r}) & \Sigma_{a,2}(\boldsymbol{r}) - D_2(\boldsymbol{r})\nabla^2 \end{bmatrix} \tag{13}$$

$$\overline{\overline{F}}(\boldsymbol{r}) = \begin{bmatrix} \nu\Sigma_{f,1}(\boldsymbol{r}) & \nu\Sigma_{f,2}(\boldsymbol{r}) \\ 0 & 0 \end{bmatrix} \tag{14}$$

$$\bar{\phi}(\boldsymbol{r}) = \begin{bmatrix} \phi_1(\boldsymbol{r}) \\ \phi_2(\boldsymbol{r}) \end{bmatrix} \tag{15}$$

then the flux and the eigenvalue can be searched for by using an iterative scheme. In the present study, the power iteration method was chosen for its simplicity and its relative efficiency (Bell and Glasstone, 1970), (Nakamura, 1977). In such a method, the flux and the eigenvalue are given by the following expressions:

$$\bar{\phi}^{(n)}(\boldsymbol{r}) = \overline{\overline{M}}^{-1}(\boldsymbol{r}) \times \frac{1}{k_{eff}^{(n-1)}} \overline{\overline{F}}(\boldsymbol{r}) \times \bar{\phi}^{(n-1)}(\boldsymbol{r}) \tag{16}$$

and

$$k_{eff}^{(n)} = \frac{\overline{\overline{F}}(\boldsymbol{r}) \times \bar{\phi}^{(n)}(\boldsymbol{r})}{\overline{\overline{F}}(\boldsymbol{r}) \times \bar{\phi}^{(n-1)}(\boldsymbol{r})} \times k_{eff}^{(n-1)} \tag{17}$$

where (n) represents the iteration number. The starting point of this method is an initial guess for $\bar{\phi}^{(0)}(\boldsymbol{r})$ and $k_{eff}^{(0)}$. In this study, the values given by SIMULATE-3 were chosen[3]. Then, a new flux distribution is calculated via Eq. (16), and subsequently a new eigenvalue is estimated via Eq. (17). This procedure is repeated until some convergence criteria regarding both the neutron flux and the eigenvalue are fulfilled. Then the results have to be scaled since Eq. (8) is a homogeneous equation. The scaling is required for comparison purposes between the static core simulator and SIMULATE-3 (the MTC estimated theoretically via the noise technique is independent of this scaling, see Section 3). The scaling factor is calculated so that the power level corresponds to the one given by SIMULATE-3 in the axially condensed reactor:

$$\int_{fuel} [\kappa_1(\boldsymbol{r})\phi_1(\boldsymbol{r}) + \kappa_2(\boldsymbol{r})\phi_2(\boldsymbol{r})]d\boldsymbol{r}\Big|_{\text{static core simulator}} = \int_{fuel} [\kappa_1(\boldsymbol{r})\phi_1(\boldsymbol{r}) + \kappa_2(\boldsymbol{r})\phi_2(\boldsymbol{r})]d\boldsymbol{r}\Big|_{\text{SIMULATE-3}} \tag{18}$$

where $\kappa_1(\boldsymbol{r})$ and $\kappa_2(\boldsymbol{r})$ are the energy release per fast and thermal fission respectively.

This static core simulator was then benchmarked against SIMULATE-3. In such a benchmark, the cross-sections used in the 2-D simulator were obviously obtained directly from the 3-D core modelled in SIMULATE-3 without any modification of the absorption cross-sections (which would have been necessary to take the leakage in the axial direction into account, as described previously (see Section 2.1)). Such a cross-section adjustment would have made the axially condensed systems significantly different with respect to the flux calculation. It is therefore expected that the eigenvalue given by the static core simulator (2-D system) will be significantly larger than the one given by SIMULATE-3 (3-D system).

The results of the benchmarking are given in Figs. 1 and 2. The peaks observed in Fig. 1 correspond to the reflector peaks, i.e. an increase of the thermal flux in the reflector region, and are also observed in the SIMULATE-3 results. Furthermore, the agreement between the static core simulator and SIMULATE-3 is very good in the fuel zone. The discrepancy is nevertheless relatively significant in the reflector zone for two main reasons. First of all, the discretisation scheme used in the static core simulator, i.e. the finite difference scheme, is known to give poor results when there are large flux gradients, such as for instance in the reflector region and close to this region. SIMULATE-3 uses a nodal diffusion model, which gives much more accurate results in such cases. Another difference between the two modelling is the number of nodes used in the calculation. In SIMULATE-3, the core is described via a 32x32 lattice, whereas the static core simulator uses a 64x64 lattice. In order to compare the results of the two calculations, the SIMULATE-3 results were simply expanded on the 64x64 grid without any interpolation, i.e. the results are spatially homogeneous on each 2x2 node. Consequently, a reflector "bundle" is actually described by 2x2 nodes in the static core simulator, whereas it is described by only 1x1 node in SIMULATE-3. Since the static

3. For the flux, the axially condensed flux given by SIMULATE-3 is actually used.

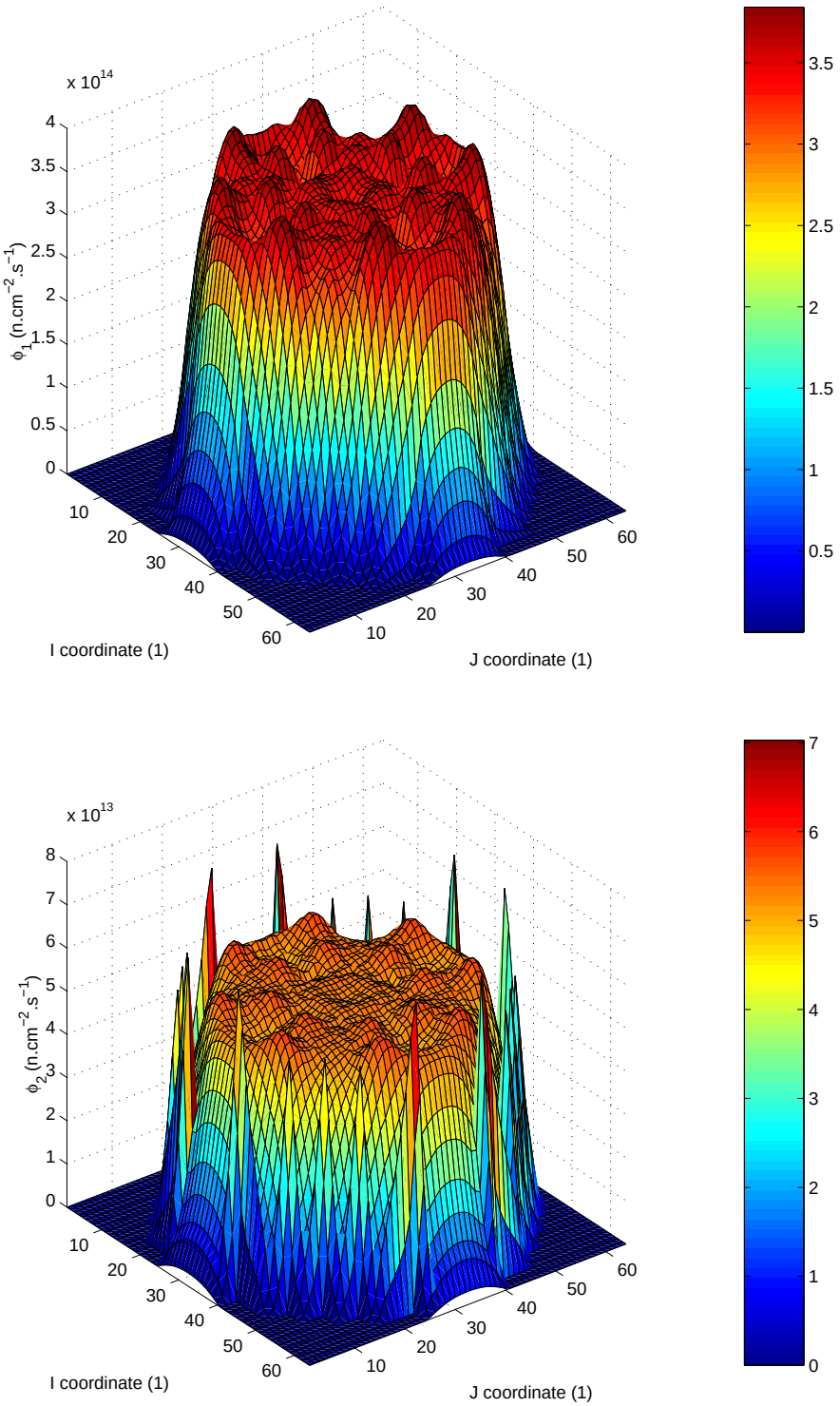

Figure 1: Static flux calculations provided by the static core simulator in the benchmark case (the fast flux is given in the upper figure, and the thermal flux is given in the lower figure)

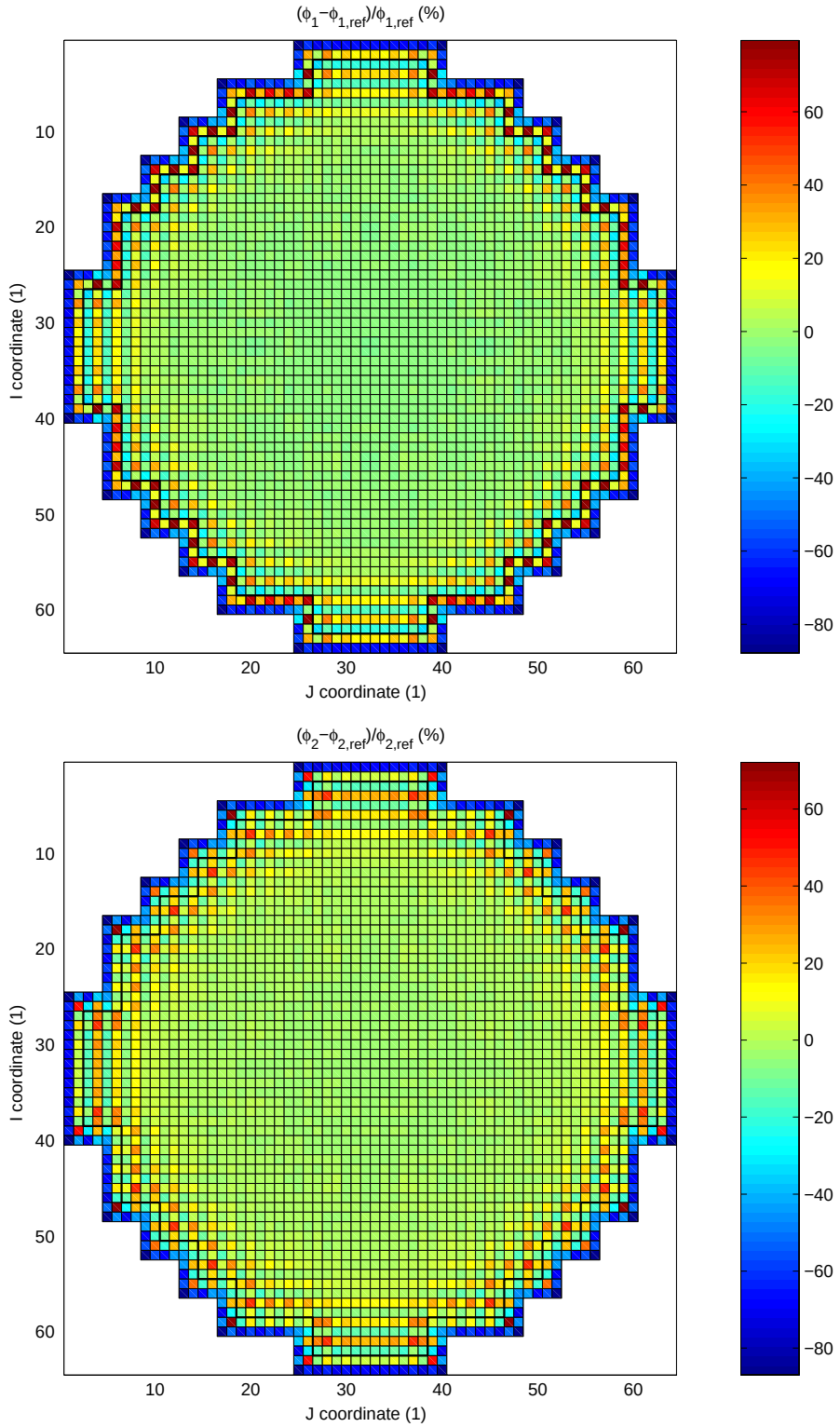

Figure 2: Relative difference in the static flux calculations between the static core simulator and SIMULATE-3 in the benchmark case, with SIMULATE-3 being considered as the reference case; the comparison of the fast flux is given in the upper figure, and the comparison of the thermal flux is given in the lower one

flux is assumed to vanish at the core boundary, big discrepancies are thus expected in the reflector region. Concerning the eigenvalue calculation, the static core simulator gives a value of 1.00332, whereas SIMULATE-3 gives a value of 0.99998. This discrepancy was expected since the static core simulator represents a 2-D system in which the axial leakage was eliminated, whereas SIMULATE-3 represents an actual 3-D system.

2.3. Description of the adjoint core simulator

As mentioned previously, the adjoint flux, together with the static flux, is needed in this theoretical investigation for the calculation of the coolant average temperature noise throughout the core (see Section 3).

In the two-group diffusion approximation, the adjoint flux is solution of the following matrix equation:

$$[\overline{\overline{D}}(\boldsymbol{r})\nabla^2 + \overline{\overline{\Sigma}}^{+}(\boldsymbol{r})] \times \begin{bmatrix} \phi_1^{+}(\boldsymbol{r}) \\ \phi_2^{+}(\boldsymbol{r}) \end{bmatrix} = 0 \tag{19}$$

where $\overline{\overline{D}}(\boldsymbol{r})$ is given by Eq. (9) and where $\overline{\overline{\Sigma}}^{+}(\boldsymbol{r})$ is the adjoint of $\overline{\overline{\Sigma}}(\boldsymbol{r})$, i.e. its transpose:

$$\overline{\overline{\Sigma}}^{+}(\boldsymbol{r}) = \begin{bmatrix} \dfrac{\nu\Sigma_{f,1}(\boldsymbol{r})}{k_{eff}} - \Sigma_{a,1}(\boldsymbol{r}) - \Sigma_{rem}(\boldsymbol{r}) & \Sigma_{rem}(\boldsymbol{r}) \\ \dfrac{\nu\Sigma_{f,2}(\boldsymbol{r})}{k_{eff}} & -\Sigma_{a,2}(\boldsymbol{r}) \end{bmatrix} \tag{20}$$

The spatial discretisation is carried out as before, i.e. by using the finite differences and the so-called "box-scheme":

$$\begin{aligned} &\frac{1}{\Delta x \cdot \Delta y} \int_{(I,J)} D_G(\boldsymbol{r})\nabla^2\phi_G^{+}(\boldsymbol{r})d\boldsymbol{r} \\ &= -\frac{(a^x_{G,I,J}\phi^{+}_{G,I,J} + b^x_{G,I,J}\phi^{+}_{G,I+1,J} + c^x_{G,I,J}\phi^{+}_{G,I-1,J})}{\Delta x} \\ &- \frac{(a^y_{G,I,J}\phi^{+}_{G,I,J} + b^y_{G,I,J}\phi^{+}_{G,I,J+1} + c^y_{G,I,J}\phi^{+}_{G,I,J-1})}{\Delta y} \end{aligned} \tag{21}$$

with the different coefficients $a^x_{G,I,J}$, $a^y_{G,I,J}$, $b^x_{G,I,J}$, $b^y_{G,I,J}$, $c^x_{G,I,J}$, and $c^y_{G,I,J}$ given previously (see Table 2 and Table 3).

The matrix equation given by Eq. (19) has to be used to determine both the two-group adjoint fluxes and the eigenvalue. In principle the eigenvalue of the direct problem should be equal to the eigenvalue of the adjoint problem. Nevertheless, due the discretisation scheme used in the calculations, it is not granted that these two eigenvalues

are still identical in the discretised problem. If the two simulators, i.e. the static and the adjoint ones, are consistent, then the two numerical eigenvalues should be very close to each other (as will be seen in the following, the two eigenvalues are actually identical). Therefore the eigenvalue calculation has to be performed simultaneously with the flux calculation, in order to verify that the difference between the two eigenvalues is negligible. This can be done as before via the so-called outer iteration that can be summarised as follows. If one rewrites Eqs. (19) and (20) as:

$$\overline{\overline{M}}^{+}(\boldsymbol{r}) \times \bar{\phi}^{+}(\boldsymbol{r}) = \frac{1}{k_{eff}^{+}} \overline{\overline{F}}^{+}(\boldsymbol{r}) \times \bar{\phi}^{+}(\boldsymbol{r}) \tag{22}$$

where $\overline{\overline{M}}^{+}(\boldsymbol{r})$ and $\overline{\overline{F}}^{+}(\boldsymbol{r})$ are the adjoint of $\overline{\overline{M}}(\boldsymbol{r})$ and $\overline{\overline{F}}(\boldsymbol{r})$ respectively, i.e. their transpose:

$$\overline{\overline{M}}^{+}(\boldsymbol{r}) = \begin{bmatrix} \Sigma_{a,1}(\boldsymbol{r}) + \Sigma_{rem}(\boldsymbol{r}) - D_1(\boldsymbol{r})\nabla^2 & -\Sigma_{rem}(\boldsymbol{r}) \\ 0 & \Sigma_{a,2}(\boldsymbol{r}) - D_2(\boldsymbol{r})\nabla^2 \end{bmatrix} \tag{23}$$

$$\overline{\overline{F}}^{+}(\boldsymbol{r}) = \begin{bmatrix} \nu\Sigma_{f,1}(\boldsymbol{r}) & 0 \\ \nu\Sigma_{f,2}(\boldsymbol{r}) & 0 \end{bmatrix} \tag{24}$$

and

$$\bar{\phi}^{+}(\boldsymbol{r}) = \begin{bmatrix} \phi_1^{+}(\boldsymbol{r}) \\ \phi_2^{+}(\boldsymbol{r}) \end{bmatrix} \tag{25}$$

then the flux and the eigenvalue can be searched for by using an iterative scheme. By using as before the power iteration method, the flux and the eigenvalue are given by the following expressions:

$$\bar{\phi}^{+(n)}(\boldsymbol{r}) = \overline{\overline{M}}^{+-1}(\boldsymbol{r}) \times \frac{1}{k_{eff}^{+(n-1)}} \overline{\overline{F}}^{+}(\boldsymbol{r}) \times \bar{\phi}^{+(n-1)}(\boldsymbol{r}) \tag{26}$$

and

$$k_{eff}^{+(n)} = \frac{\overline{\overline{F}}^{+}(\boldsymbol{r}) \times \bar{\phi}^{+(n)}(\boldsymbol{r})}{\overline{\overline{F}}^{+}(\boldsymbol{r}) \times \bar{\phi}^{+(n-1)}(\boldsymbol{r})} \times k_{eff}^{+(n-1)} \tag{27}$$

where (n) represents the iteration number. The starting point of this method is an initial guess for $\bar{\phi}^{+(0)}(\boldsymbol{r})$ and $k_{eff}^{+(0)}$. In this study, the values given by SIMULATE-3 were chosen[4]. Then, a new adjoint flux distribution is calculated via Eq. (26), and subsequently a new eigenvalue is estimated via Eq. (27). This procedure is repeated until some conver-

gence criteria regarding both the neutron flux and the eigenvalue are fulfilled. Then the results have to be scaled since Eq. (19) is a homogeneous equation. The scaling is required for comparison purposes between the adjoint core simulator and SIMULATE-3 (the MTC estimated theoretically via the noise technique is independent of this scaling, see Section 3). The scaling factor is calculated so that the volume integral of the fast adjoint flux is equal to unity:

$$\frac{1}{V_{core}} \int_{core} \phi_1^+(\boldsymbol{r}) d\boldsymbol{r} = 1 \tag{28}$$

where V_{core} is the volume of the core (without reflector, i.e. only the fuel region).

This adjoint core simulator was then benchmarked against SIMULATE-3. In such a benchmark, the cross-sections used in the 2-D simulator were once again obtained directly from the 3-D core modelled in SIMULATE-3 without any modification of the absorption cross-sections. It is therefore expected that the eigenvalue given by the adjoint core simulator (2-D system) will be significantly larger than the one given by SIMULATE-3 (3-D system).

The results of the benchmarking are given in Figs. 3 and 4. As can be seen in these figures, the agreement between the adjoint core simulator and SIMULATE-3 is very good in the fuel zone, whereas the discrepancy is significant in the reflector zone. The same reasons as the ones presented for the static core simulator could explain this discrepancy, i.e. the difference in the spatial discretisation schemes between SIMULATE-3 and the adjoint core simulator, and the different number of nodes used for the calculations. Concerning the eigenvalue calculation, the adjoint core simulator gives a value of 1.00332, whereas SIMULATE-3 gives a value of 0.99998 for k_{eff}^+. These values are identical to the ones given by the static direct calculations. The discrepancy between the SIMULATE-3 and the adjoint core simulator results was expected since the adjoint core simulator represents a 2-D system in which the axial leakage was eliminated, whereas SIMULATE-3 represents an actual 3-D system.

2.4. Description of the noise simulator

The neutron noise simulator was extensively described in (Pázsit et al, 2000) and (Pázsit et al, 2001). In the following, only the main characteristics of this neutron noise simulator are recalled.

The neutron noise simulator is able to calculate the spatial distribution of the neutron noise induced by any given spatially distributed or localised noise sources. Several types of noise sources can be simultaneously investigated, i.e. a perturbation of the macroscopic absorption cross-section (fast and/or thermal), and/or a perturbation of the macroscopic removal cross-section, and/or a perturbation of the macroscopic fission cross-section (fast and/or thermal). The neutron noise simulator is able to model the noise sources of the “absorber of variable strength” type (the so-called reactor

4. For the adjoint flux, the axially condensed adjoint flux given by SIMULATE-3 is actually used.

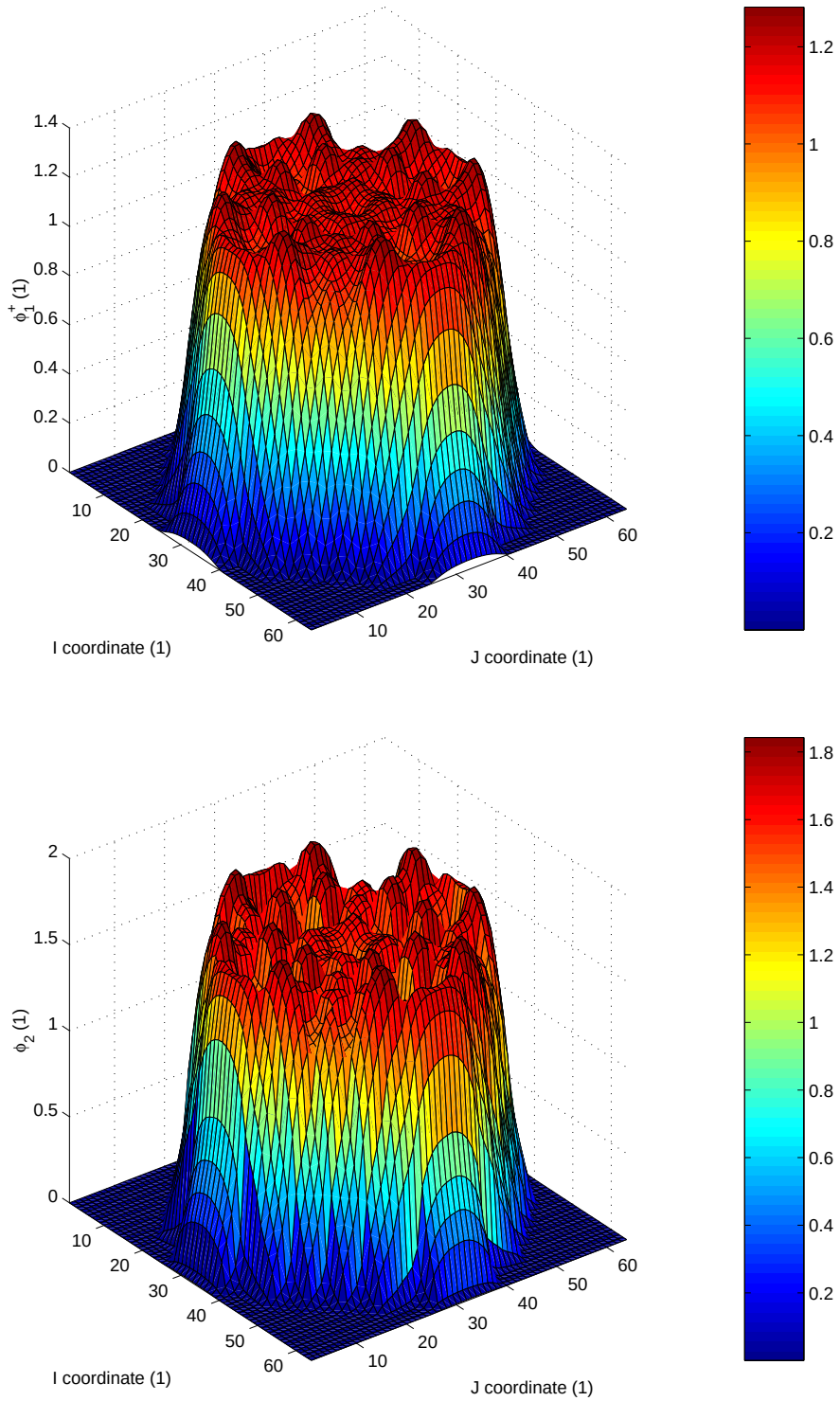

Figure 3: Adjoint flux calculations provided by the static core simulator in the benchmark case (the fast flux is given in the upper figure, and the thermal flux is given in the lower figure)

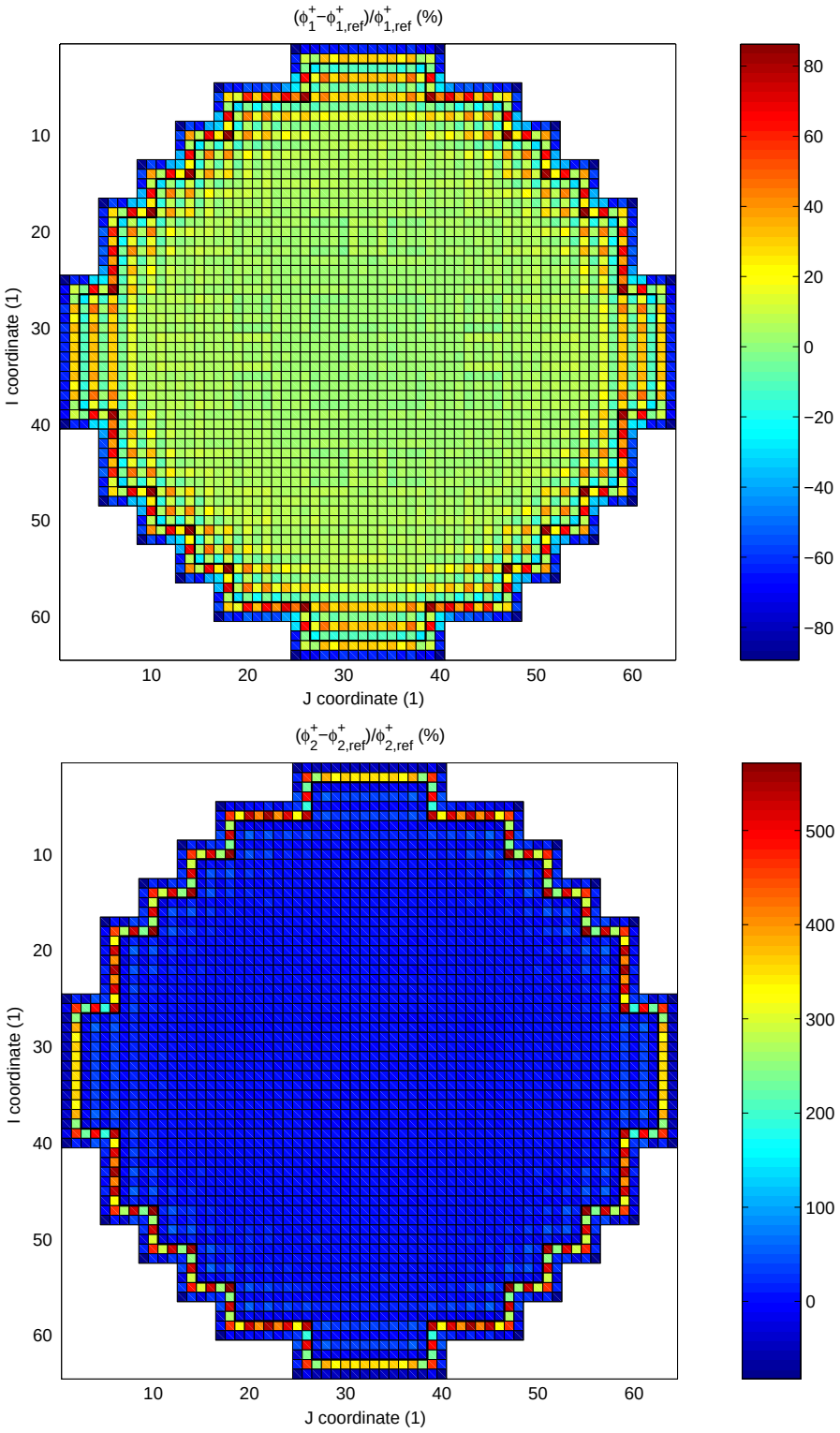

Figure 4: Relative difference in the adjoint flux calculations between the adjoint core simulator and SIMULATE-3 in the benchmark case, with SIMULATE-3 being considered as the reference case; the comparison of the fast adjoint is given in the upper figure, and the comparison of the thermal adjoint is given in the lower one

oscillator). The simulator cannot model noise sources of the "moving absorber" type. Furthermore, the calculations are directly performed in the frequency domain.

If the noise source is a point source of unit strength, the neutron noise simulator actually estimates the 2-D 2-group discretised Green's function $G_{XS \to i}(\boldsymbol{r}, \boldsymbol{r}', \omega)$, the index $i = 1, 2$ representing the fast and thermal groups respectively. More specifically, these transfer functions give the flux noise $\delta\phi_i$ in $\boldsymbol{r}$ and at a frequency $f = \omega/2\pi$ induced by a unit cross-section noise source $\delta XS = 1$ located at $\boldsymbol{r}'$ at the same frequency.

In the linear two-group diffusion theory, the neutron noise can be expressed as a solution of the following matrix equation:

$$[\bar{\bar{D}}(\boldsymbol{r})\nabla^2 + \bar{\bar{\Sigma}}(\boldsymbol{r}, \omega)] \times \begin{bmatrix} \delta\phi_1(\boldsymbol{r}, \omega) \\ \delta\phi_2(\boldsymbol{r}, \omega) \end{bmatrix}$$

$$= \bar{\phi}_{rem}(\boldsymbol{r})\delta\Sigma_{rem}(\boldsymbol{r}, \omega) + \bar{\bar{\phi}}_a(\boldsymbol{r}) \begin{bmatrix} \delta\Sigma_{a,1}(\boldsymbol{r}, \omega) \\ \delta\Sigma_{a,2}(\boldsymbol{r}, \omega) \end{bmatrix} + \bar{\bar{\phi}}_f(\boldsymbol{r}, \omega) \begin{bmatrix} \delta\nu\Sigma_{f,1}(\boldsymbol{r}, \omega) \\ \delta\nu\Sigma_{f,2}(\boldsymbol{r}, \omega) \end{bmatrix} \tag{29}$$

where the different matrices/vector are given as:

$$\bar{\bar{\Sigma}}(\boldsymbol{r}, \omega) = \begin{bmatrix} -\Sigma_1(\boldsymbol{r}, \omega) & \nu\Sigma_{f,2}(\boldsymbol{r}, \omega) \\ \Sigma_{rem}(\boldsymbol{r}) & -\Sigma_{a,2}(\boldsymbol{r}, \omega) \end{bmatrix} \tag{30}$$

$$\bar{\phi}_{rem}(\boldsymbol{r}) = \begin{bmatrix} \phi_1(\boldsymbol{r}) \\ -\phi_1(\boldsymbol{r}) \end{bmatrix} \tag{31}$$

$$\bar{\bar{\phi}}_a(\boldsymbol{r}) = \begin{bmatrix} \phi_1(\boldsymbol{r}) & 0 \\ 0 & \phi_2(\boldsymbol{r}) \end{bmatrix} \tag{32}$$

$$\bar{\bar{\phi}}_f(\boldsymbol{r}, \omega) = \begin{bmatrix} -\phi_1(\boldsymbol{r})\left(1 - \dfrac{i\omega\beta_{eff}}{i\omega + \lambda}\right) & -\phi_2(\boldsymbol{r})\left(1 - \dfrac{i\omega\beta_{eff}}{i\omega + \lambda}\right) \\ 0 & 0 \end{bmatrix} \tag{33}$$

and the different coefficients are defined as:

$$\Sigma_1(\boldsymbol{r}, \omega) = \Sigma_{a,1}(\boldsymbol{r}) + \frac{i\omega}{v_1} + \Sigma_{rem}(\boldsymbol{r}) - \nu\Sigma_{f,1}(\boldsymbol{r})\left(1 - \frac{i\omega\beta_{eff}}{i\omega + \lambda}\right) \tag{34}$$

$$\nu\Sigma_{f,2}(\boldsymbol{r}, \omega) = \nu\Sigma_{f,2}(\boldsymbol{r})\left(1 - \frac{i\omega\beta_{eff}}{i\omega + \lambda}\right) \tag{35}$$

$$\Sigma_{a,2}(\boldsymbol{r},\omega) = \Sigma_{a,2}(\boldsymbol{r}) + \frac{i\omega}{v_2} \tag{36}$$

The matrix $\overline{\overline{D}}(\boldsymbol{r})$ is identical to the one given by Eq. (9).

The spatial discretisation is carried out as before, i.e. by using the finite differences and the so-called "box-scheme":

$$\frac{1}{\Delta x \cdot \Delta y} \int_{(I,J)} D_G(\boldsymbol{r}) \nabla^2 \delta\phi_G(\boldsymbol{r},\omega) d\boldsymbol{r} \tag{37}$$

$$= -\frac{(a^x_{G,I,J}\delta\phi_{G,I,J}(\omega) + b^x_{G,I,J}\delta\phi_{G,I+1,J}(\omega) + c^x_{G,I,J}\delta\phi_{G,I-1,J}(\omega))}{\Delta x}$$

$$-\frac{(a^y_{G,I,J}\delta\phi_{G,I,J}(\omega) + b^y_{G,I,J}\delta\phi_{G,I,J+1}(\omega) + c^y_{G,I,J}\delta\phi_{G,I,J-1}(\omega))}{\Delta y}$$

with the different coefficients $a^x_{G,I,J}$, $a^y_{G,I,J}$, $b^x_{G,I,J}$, $b^y_{G,I,J}$, $c^x_{G,I,J}$, and $c^y_{G,I,J}$ given previously (see Table 2 and Table 3).

Unlike the calculation of the static flux and the adjoint flux, the equation giving the neutron noise, i.e. Eq. (29), is not a homogeneous equation, but represents a source problem. Consequently, the discretised form of the matrix $[\overline{\overline{D}}(\boldsymbol{r})\nabla^2 + \overline{\overline{\phi}}(\boldsymbol{r},\omega)]$ can be directly inverted, and the flux noise calculated accordingly.

Even if Eq. (29) was written for any kind of noise sources, only one type will be investigated in the MTC study. In order to determine which macroscopic cross-section is the most sensitive to the coolant temperature, two SIMULATE-3 calculations were run: the first one at the nominal operating conditions corresponding to the operational point described previously, i.e. on May 5th, 1999, and the second one for the same burnup but with a core inlet temperature increased by +5 °F (2.78 °C). For this second calculation, the fuel temperature was kept equal to the one estimated during the first calculation, and so were the main fission products (promethium, samarium, iodine, and xenon). Three quantities are then studied (all the 0-D parameters are directly obtained from SIMULATE-3):

- The relative variation (in percent) of each macroscopic cross-section defined as:

$$\Delta XS_{\text{0-D}} = \frac{XS_{\text{0-D},\,T_{in}+5} - XS_{\text{0-D},\,T_{in}}}{XS_{\text{0-D},\,T_{in}}} \times 100 \tag{38}$$

- The relative variation (in percent) of the corresponding reaction rate defined as:

$$\Delta RR_{\text{0-D}} = \frac{XS_{\text{0-D},\,T_{in}+5} \times \phi_{G,\,\text{0-D},\,T_{in}+5} - XS_{\text{0-D},\,T_{in}} \times \phi_{G,\,\text{0-D},\,T_{in}}}{XS_{\text{0-D},\,T_{in}} \times \phi_{G,\,\text{0-D},\,T_{in}}} \times 100 \tag{39}$$

where G is the group index associated with the cross-section variation which is studied;

- The corresponding reactivity variation (in pcm) for each different type of cross-section given as:

$$\Delta\rho = \frac{k_{eff,\,T_{in}+5} - k_{eff,\,T_{in}}}{k^2_{eff,\,T_{in}}} \times 10^5 \tag{40}$$

where the effective multiplication factor, at a given core inlet temperature, is evaluated according to the following formula:

$$k_{eff} = \frac{\nu\Sigma_{f,\,2,\,0\text{-D}} + \nu\Sigma_{f,\,1,\,0\text{-D}} \times \dfrac{\phi_{1,\,0\text{-D}}}{\phi_{2,\,0\text{-D}}}}{\Sigma_{a,\,2,\,0\text{-D}}} \tag{41}$$

$$\times \frac{\Sigma_{rem,\,0\text{-D}}}{\Sigma_{a,\,1,\,0\text{-D}} + \Sigma_{rem,\,0\text{-D}}} \times \frac{1}{1 + \dfrac{D_{1,\,0\text{-D}}}{\Sigma_{a,\,1,\,0\text{-D}} + \Sigma_{rem,\,0\text{-D}}} \times B^2_{g,\,1,\,0\text{-D}}} \times \frac{1}{1 + \dfrac{D_{2,\,0\text{-D}}}{\Sigma_{a,\,2,\,0\text{-D}}} \times B^2_{g,\,2,\,0\text{-D}}}$$

All the symbols in Eq. (41) have their usual meaning. When evaluating Eq. (41), the effect of the change of each cross-section was studied separately, i.e. $k_{eff,\,T_{in}+5}$ was estimated by using the value of this specific cross-section at $T_{in} + 5$, all the other cross-sections taken at T_{in}.

The results are summarised in the following Table 4. As can be seen, the cross-section that has the largest reactivity effect is the macroscopic removal cross-section. Therefore in the following, the noise source will be assumed to be a macroscopic removal cross-section noise, i.e. the noise simulator will calculate the transfer function from the macroscopic removal cross-section noise source to the induced neutron noise.

Table 4: Effect of a variation of the core inlet temperature (+5 °F) on each of the macroscopic cross-sections

$XS_{0\text{-D}}$	$\Sigma_{rem,\,0\text{-D}}$	$\Sigma_{a,\,1,\,0\text{-D}}$	$\Sigma_{a,\,2,\,0\text{-D}}$	$\nu\Sigma_{f,\,1,\,0\text{-D}}$	$\nu\Sigma_{f,\,2,\,0\text{-D}}$
$\Delta XS_{0\text{-D}}$ (%)	-0.94	-0.15	-0.21	-0.17	-0.13
$\Delta RR_{0\text{-D}}$ (%)	-0.21	0.59	-0.21	0.57	-0.14
$\Delta\rho$ (pcm)	-414	60	207	-35	-105

The neutron noise simulator was already benchmarked previously during Stage 7 of the SKI project (Pázsit et al, 2001). In the following, only the case of a macroscopic removal cross-section noise is presented. The layout of the core in this benchmark is representative of the Swedish BWR Forsmark-1. The core was assumed to be a two-region system (fuel + reflector), in which each region was spatially homogeneous. The material constants, the point-kinetic parameters and the flux data were obtained from a

generic General Electric BWR/6. At that time, the flux was not recalculated with a dicretisation scheme compatible with the finite difference scheme, so that the macroscopic cross-sections were slightly adjusted in each node in order to fulfil the balance equations in each node with respect to the finite difference scheme (as written in (Pázsit et al, 2001), this adjustment was only noticeable close to and in the reflector region). The noise source was located in the middle of the core. Since the core was roughly homogeneous, an analytical solution could be estimated and was used as a reference solution. The results of this benchmark are presented in Figs. 5 and 6. Since the noise source was located in the middle of the core, the results are rotational-invariant around the *z*-axis crossing the core centre. Therefore only the radial dependence of the fluxes is plotted in the Figures.

It can be noticed that the agreement between the numerical solution and the analytical one is very good for both the magnitude and the phase of the induced neutron noise. Since the noise simulator calculates a spatially-averaged flux noise over each node, the analytical solution was also averaged over each node, so that both solutions could be directly compared. The first point of the numerical solution (from the core centre) represents therefore the flux noise in the node where the noise source is located. The analytical solution gives obviously a different solution in this node, and thus the first point of the analytical solution was systematically disregarded. Finally, due to the cross-section adjustment, which is noticeable only around the reflector region, the accuracy close to the reflector deteriorates slightly, but remains still acceptable. Another reason explaining this discrepancy lies with the fact that the analytical solution does not take any reflector into account.

3. Derivation of the MTC noise estimators for 2-D 2-group heterogeneous systems

According to the recent American Standard (ANSI, 1997), the MTC is defined as the variation of reactivity induced by a variation of the inlet temperature of the core, divided by the variation of the core average of the coolant temperature. In the noise analysis technique, the MTC can therefore be inferred from the reactivity noise and the core average coolant temperature noise. In the following, expressions for these two quantities are derived in the two-group formalism. The theoretical two-group MTC noise estimators are then derived.

3.1. Calculation of the reactivity noise in multigroup perturbation theory

In the following, the reactivity noise induced by a given noise source is presented. As mentioned previously, emphasis is put on the case of a macroscopic removal cross-section noise source, but the derivation is presented for a much more general case, i.e. any type of noise source can be applied.

The starting point is to write the multigroup direct equations of the unperturbed system in the diffusion approximation:

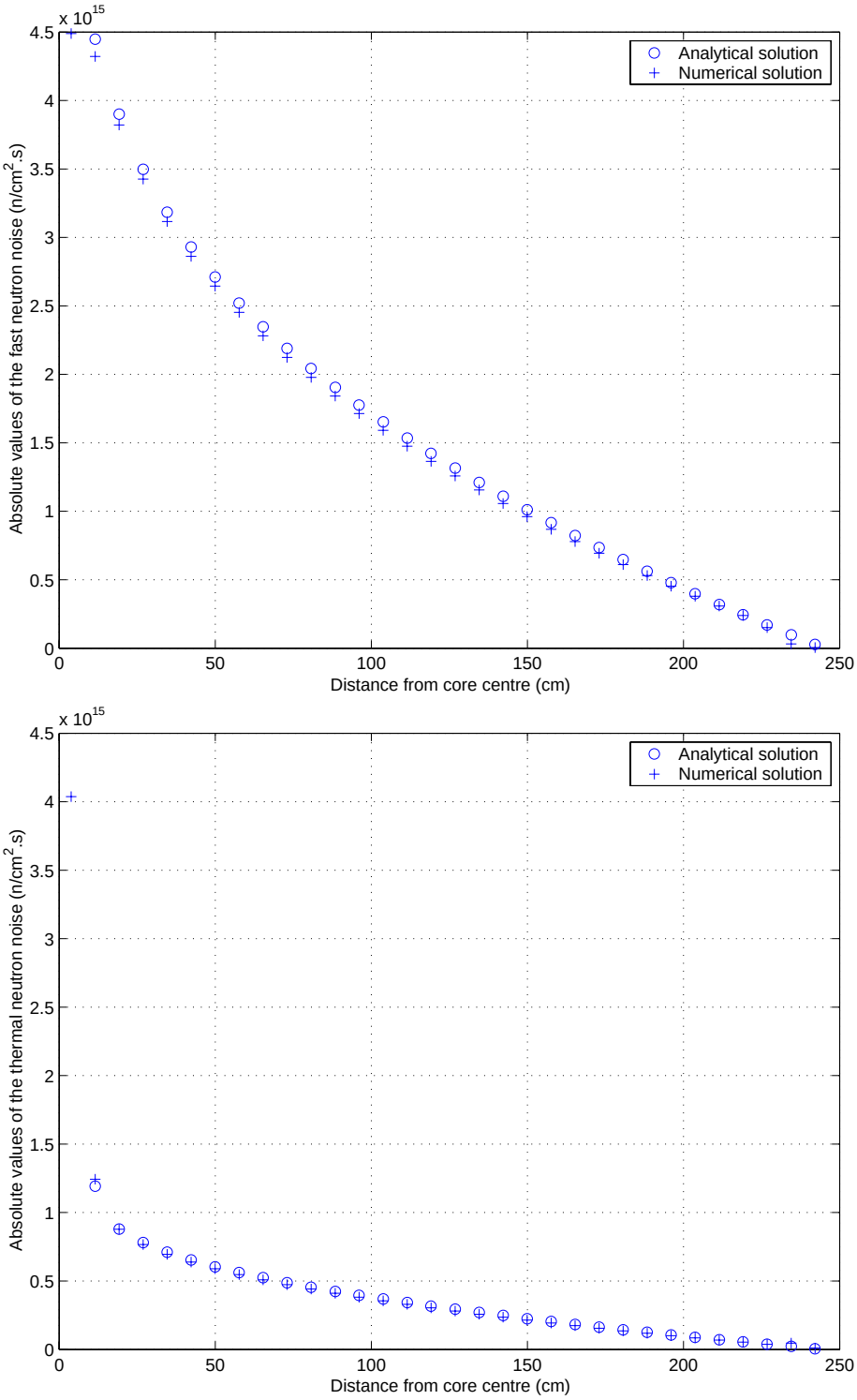

Figure 5: Comparison of the magnitude of the flux noise calculations between the neutron noise simulator and the reference solution in the benchmark case; the comparison of the fast noise is given in the upper figure, and the comparison of the thermal noise is given in the lower one

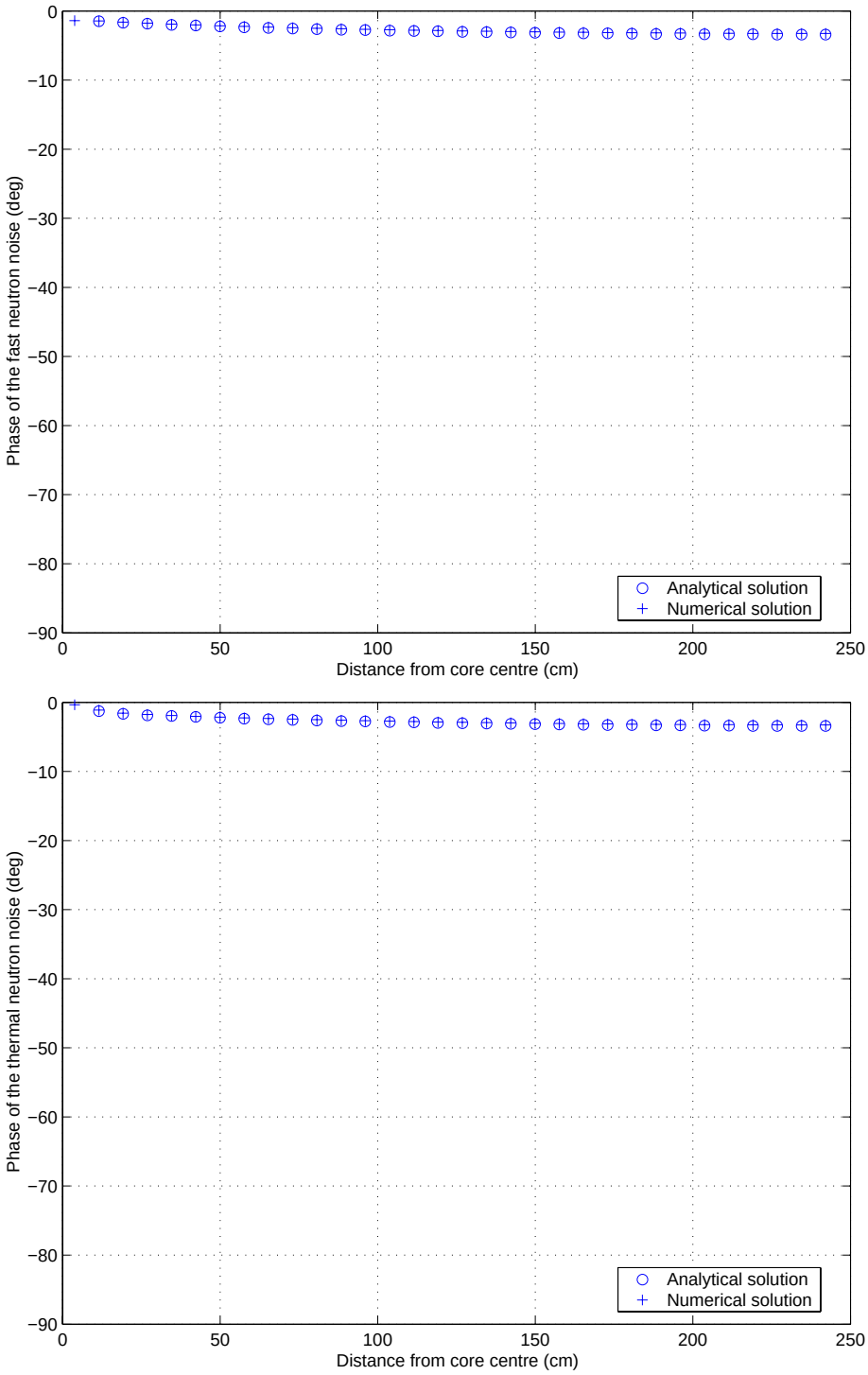

Figure 6: Comparison of the phase of the flux noise calculations between the neutron noise simulator and the reference solution in the benchmark case; the comparison of the fast noise is given in the upper figure, and the comparison of the thermal noise is given in the lower one

$$-\nabla \cdot D_G(\boldsymbol{r})\nabla\phi_G(\boldsymbol{r}) + \Sigma_{0,\,G}(\boldsymbol{r})\phi_G(\boldsymbol{r}) \tag{42}$$

$$= \sum_{G'}\Sigma_{G'\to G}(\boldsymbol{r})\phi_{G'}(\boldsymbol{r}) + \sum_{G'}\frac{\nu\Sigma_{f,\,G'\to G}(\boldsymbol{r})}{k_{eff}}\phi_{G'}(\boldsymbol{r})$$

with

$$\Sigma_{0,\,G}(\boldsymbol{r}) = \Sigma_{a,\,G}(\boldsymbol{r}) + \sum_{G'}\Sigma_{G\to G'}(\boldsymbol{r}) \tag{43}$$

$$\nu\Sigma_{f,\,G'\to G}(\boldsymbol{r}) = \chi_G\nu\Sigma_{f,\,G'}(\boldsymbol{r}) \tag{44}$$

All the symbols have their usual meaning.

The corresponding adjoint equations read as:

$$-\nabla \cdot D_G(\boldsymbol{r})\nabla\overset{+}{\phi}_G(\boldsymbol{r}) + \Sigma_{0,\,G}(\boldsymbol{r})\overset{+}{\phi}_G(\boldsymbol{r}) \tag{45}$$

$$= \sum_{G'}\Sigma_{G\to G'}(\boldsymbol{r})\overset{+}{\phi}_{G'}(\boldsymbol{r}) + \sum_{G'}\frac{\nu\Sigma_{f,\,G\to G'}(\boldsymbol{r})}{\overset{+}{k}_{eff}}\overset{+}{\phi}_{G'}(\boldsymbol{r})$$

The direct equations for the perturbed system are then given by:

$$-\nabla \cdot \overset{*}{D}_G(\boldsymbol{r}, t)\nabla\overset{*}{\phi}_G(\boldsymbol{r}, t) + \overset{*}{\Sigma}_{0,\,G}(\boldsymbol{r}, t)\overset{*}{\phi}_G(\boldsymbol{r}, t) \tag{46}$$

$$= \sum_{G'}\overset{*}{\Sigma}_{G'\to G}(\boldsymbol{r}, t)\overset{*}{\phi}_{G'}(\boldsymbol{r}, t) + \sum_{G'}\frac{\nu\overset{*}{\Sigma}_{f,\,G'\to G}(\boldsymbol{r}, t)}{\overset{*}{k}_{eff}}\overset{*}{\phi}_{G'}(\boldsymbol{r}, t)$$

with the perturbed quantities defined by the following generic formulation:

$$\overset{*}{P}(\boldsymbol{r}, t) = P(\boldsymbol{r}) + \delta P(\boldsymbol{r}, t) \tag{47}$$

where P represents any of the following parameters: D_G, $\Sigma_{0,\,G}$, $\Sigma_{G'\to G}$, $\nu\Sigma_{f,\,G'\to G}$, ϕ_G, and k_{eff}.

Multiplying Eq. (46) by $\overset{+}{\phi}_G(\boldsymbol{r})$, Eq. (45) by $\overset{*}{\phi}_G(\boldsymbol{r})$, substracting these two quantities, and applying the Stokes-Ostrogradski theorem leads to (Bell and Glasstone, 1970):

$$\int [-\phi_G^+(\boldsymbol{r})\nabla \cdot \delta D_G(\boldsymbol{r}, t)\nabla \phi_G^*(\boldsymbol{r}, t) + \phi_G^+(\boldsymbol{r})\delta\Sigma_{0,\,G}(\boldsymbol{r}, t)\phi_G^*(\boldsymbol{r}, t)]d\boldsymbol{r} \tag{48}$$

$$= \int \Bigg[\sum_{G'} \phi_G^+(\boldsymbol{r})\delta\Sigma_{G' \to G}(\boldsymbol{r}, t)\phi_{G'}^*(\boldsymbol{r}, t)$$

$$+ \sum_{G'} \phi_G^+(\boldsymbol{r}) \frac{\nu\Sigma_{f,\,G' \to G}^*(\boldsymbol{r}, t)}{k_{eff}^*} \phi_{G'}^*(\boldsymbol{r}, t) - \sum_{G'} \phi_G^*(\boldsymbol{r}) \frac{\nu\Sigma_{f,\,G \to G'}(\boldsymbol{r}, t)}{k_{eff}^+} \phi_{G'}^+(\boldsymbol{r}, t) \Bigg] d\boldsymbol{r}$$

Summing over all the groups G, and neglecting the second-order terms gives:

$$\delta\rho(t) = \frac{\delta k_{eff}}{k_{eff}^2} = \frac{N}{\sum_G \int \Big[\sum_{G'} \nu\Sigma_{f,\,G' \to G}(\boldsymbol{r})\phi_G^+(\boldsymbol{r})\phi_{G'}(\boldsymbol{r}) \Big] d\boldsymbol{r}} \tag{49}$$

with N being equal to

$$N = \sum_G \int \Bigg\{ \phi_G^+(\boldsymbol{r})\nabla \cdot \delta D_G(\boldsymbol{r}, t)\nabla \phi_G(\boldsymbol{r}) - \delta\Sigma_{0,\,G}(\boldsymbol{r}, t)\phi_G^+(\boldsymbol{r})\phi_G(\boldsymbol{r}) \tag{50}$$

$$+ \sum_{G'} \delta\Sigma_{G' \to G}(\boldsymbol{r}, t)\phi_G^+(\boldsymbol{r})\phi_{G'}(\boldsymbol{r})$$

$$+ \sum_{G'} \left[\frac{\delta\nu\Sigma_{f,\,G' \to G}(\boldsymbol{r}, t)}{k_{eff}} + \nu\Sigma_{f,\,G' \to G}(\boldsymbol{r}) \times \left(\frac{1}{k_{eff}} - \frac{1}{k_{eff}^+} \right) \right] \phi_G^+(\boldsymbol{r})\phi_{G'}(\boldsymbol{r}) \Bigg\} d\boldsymbol{r}$$

In two-group theory, it is common practice to assume that $\delta D_G(\boldsymbol{r}, t) \approx 0, \forall(\boldsymbol{r}, t)$, $\nu\Sigma_{f,\,1 \to 2}(\boldsymbol{r}) \approx 0, \forall \boldsymbol{r}$ and $\nu\Sigma_{f,\,2 \to 2}(\boldsymbol{r}) \approx 0, \forall \boldsymbol{r}$. In principle, one should also have $k_{eff}^+ = k_{eff}$. Nevertheless, it is not granted that the two discretised problems, i.e. the direct one and the adjoint one, will give the same eigenvalue. Running the two simulators (the direct and the adjoint) seems to prove that the same eigenvalue is reached in the power iteration method. Therefore, one will assume anyway in the following that $k_{eff}^+ \approx k_{eff}$. The Fourier transform of Eq. (50) gives then the following results:

- For a macroscopic removal cross-section noise source:

$$\delta\rho(\omega) = \frac{\int -\delta\Sigma_{rem}(\boldsymbol{r}, \omega)[\phi_1^+(\boldsymbol{r})\phi_1(\boldsymbol{r}) - \phi_2^+(\boldsymbol{r})\phi_1(\boldsymbol{r})]d\boldsymbol{r}}{\int [\nu\Sigma_{f,\,1 \to 1}(\boldsymbol{r})\phi_1^+(\boldsymbol{r})\phi_1(\boldsymbol{r}) + \nu\Sigma_{f,\,2 \to 1}(\boldsymbol{r})\phi_1^+(\boldsymbol{r})\phi_2(\boldsymbol{r})]d\boldsymbol{r}} \tag{51}$$

- For a macroscopic fast absorption cross-section noise source:

$$\delta\rho(\omega) = \frac{\int -\delta\Sigma_{a,1}(\boldsymbol{r},\omega)\phi_1^+(\boldsymbol{r})\phi_1(\boldsymbol{r})d\boldsymbol{r}}{\int [\nu\Sigma_{f,1\to 1}(\boldsymbol{r})\phi_1^+(\boldsymbol{r})\phi_1(\boldsymbol{r}) + \nu\Sigma_{f,2\to 1}(\boldsymbol{r})\phi_1^+(\boldsymbol{r})\phi_2(\boldsymbol{r})]d\boldsymbol{r}} \tag{52}$$

- For a macroscopic thermal absorption cross-section noise source:

$$\delta\rho(\omega) = \frac{\int -\delta\Sigma_{a,2}(\boldsymbol{r},\omega)\phi_2^+(\boldsymbol{r})\phi_2(\boldsymbol{r})d\boldsymbol{r}}{\int [\nu\Sigma_{f,1\to 1}(\boldsymbol{r})\phi_1^+(\boldsymbol{r})\phi_1(\boldsymbol{r}) + \nu\Sigma_{f,2\to 1}(\boldsymbol{r})\phi_1^+(\boldsymbol{r})\phi_2(\boldsymbol{r})]d\boldsymbol{r}} \tag{53}$$

- For a macroscopic fast fission cross-section noise source:

$$\delta\rho(\omega) = \frac{\frac{1}{k_{eff}}\int \delta\nu\Sigma_{f,1\to 1}(\boldsymbol{r},\omega)\phi_1^+(\boldsymbol{r})\phi_1(\boldsymbol{r})d\boldsymbol{r}}{\int [\nu\Sigma_{f,1\to 1}(\boldsymbol{r})\phi_1^+(\boldsymbol{r})\phi_1(\boldsymbol{r}) + \nu\Sigma_{f,2\to 1}(\boldsymbol{r})\phi_1^+(\boldsymbol{r})\phi_2(\boldsymbol{r})]d\boldsymbol{r}} \tag{54}$$

- For a macroscopic thermal fission cross-section noise source:

$$\delta\rho(\omega) = \frac{\frac{1}{k_{eff}}\int \delta\nu\Sigma_{f,2\to 1}(\boldsymbol{r},\omega)\phi_1^+(\boldsymbol{r})\phi_2(\boldsymbol{r})d\boldsymbol{r}}{\int [\nu\Sigma_{f,1\to 1}(\boldsymbol{r})\phi_1^+(\boldsymbol{r})\phi_1(\boldsymbol{r}) + \nu\Sigma_{f,2\to 1}(\boldsymbol{r})\phi_1^+(\boldsymbol{r})\phi_2(\boldsymbol{r})]d\boldsymbol{r}} \tag{55}$$

Regarding now the MTC, its definition allows writing in the frequency domain:

$$\delta\rho(\omega) = MTC \times \delta T_m^{ave}(\omega) \tag{56}$$

In the following, one will assume that there is proportionality between the coolant temperature noise and the macroscopic cross-section noise via a frequency- and space-independent coefficient K as follows:

$$\delta T_m(\boldsymbol{r},\omega) = K \times \delta XS(\boldsymbol{r},\omega) \tag{57}$$

If the macroscopic cross-section noise is spatially homogeneous (homogeneous temperature noise), i.e. $\delta XS(\boldsymbol{r},\omega) = \delta XS^{ave}(\omega)$, $\forall \boldsymbol{r}$, the MTC can be easily estimated by using one of Eqs. (51) - (55) depending on which type of noise source is studied. One thus gets:

$$MTC = \frac{1}{K}\frac{\int w_{\Delta XS}(\boldsymbol{r})d\boldsymbol{r}}{\int [\nu\Sigma_{f,1\to 1}(\boldsymbol{r})\phi_1^+(\boldsymbol{r})\phi_1(\boldsymbol{r}) + \nu\Sigma_{f,2\to 1}(\boldsymbol{r})\phi_1^+(\boldsymbol{r})\phi_2(\boldsymbol{r})]d\boldsymbol{r}} \tag{58}$$

with the following function $w_{\Delta XS}(\boldsymbol{r})$:

- in case of a macroscopic removal cross-section noise source:

$$w_{\Delta\Sigma_{rem}}(\boldsymbol{r}) = -[\phi_1^+(\boldsymbol{r})\phi_1(\boldsymbol{r}) - \phi_2^+(\boldsymbol{r})\phi_1(\boldsymbol{r})] \tag{59}$$

- in case of a macroscopic fast absorption cross-section noise source:

$$w_{\Delta\Sigma_{a,1}}(\boldsymbol{r}) = -\phi_1^+(\boldsymbol{r})\phi_1(\boldsymbol{r}) \tag{60}$$

- in case of a macroscopic thermal absorption cross-section noise source:

$$w_{\Delta\Sigma_{a,2}}(\boldsymbol{r}) = -\phi_2^+(\boldsymbol{r})\phi_2(\boldsymbol{r}) \tag{61}$$

- in case of a macroscopic fast fission cross-section noise source:

$$w_{\Delta\nu\Sigma_{f,1}}(\boldsymbol{r}) = \frac{1}{k_{eff}}\phi_1^+(\boldsymbol{r})\phi_1(\boldsymbol{r}) \tag{62}$$

- in case of a macroscopic thermal fission cross-section noise source:

$$w_{\Delta\nu\Sigma_{f,2}}(\boldsymbol{r}) = \frac{1}{k_{eff}}\phi_1^+(\boldsymbol{r})\phi_2(\boldsymbol{r}) \tag{63}$$

If the macroscopic cross-section noise is not spatially homogeneous (heterogeneous temperature noise), the MTC should nevertheless remain identical to the one calculated beforehand (the MTC is independent of the structure of the temperature noise throughout the core). This leads to the fact that the core average macroscopic cross-section noise and the core average temperature noise should be calculated by using $w_{\Delta XS}(\boldsymbol{r})$ as a weighting function as follows:

$$\delta XS^{ave}(\omega) = \frac{\int \delta XS(\boldsymbol{r},\omega) w_{\Delta XS}(\boldsymbol{r}) d\boldsymbol{r}}{\int w_{\Delta XS}(\boldsymbol{r}) d\boldsymbol{r}} \tag{64}$$

and

$$\delta T_m^{ave}(\omega) = \frac{\int \delta T_m(\boldsymbol{r},\omega) w_{\Delta XS}(\boldsymbol{r}) d\boldsymbol{r}}{\int w_{\Delta XS}(\boldsymbol{r}) d\boldsymbol{r}} \tag{65}$$

3.2. Calibration of the noise simulator results to the SIMULATE-3 results

The MTC which has to be considered as a reference value is the one given by SIMULATE-3 (see Section 2.1). The results of the noise analysis technique can be properly scaled to this reference value by adjusting the previous coefficient K. By rewriting Eq. (58), one gets:

$$K = \frac{1}{MTC} \frac{\int w_{\Delta XS}(\boldsymbol{r}) d\boldsymbol{r}}{\int [\nu\Sigma_{f,1\to 1}(\boldsymbol{r})\phi_1^+(\boldsymbol{r})\phi_1(\boldsymbol{r}) + \nu\Sigma_{f,2\to 1}(\boldsymbol{r})\phi_1^+(\boldsymbol{r})\phi_2(\boldsymbol{r})] d\boldsymbol{r}} \tag{66}$$

Depending on the noise source type, the weighting function $w_{\Delta XS}(\boldsymbol{r})$ is different, and therefore the coefficient K differs, as shown in Table 5.

Table 5: Value of the coefficient K depending on the noise source type

noise source type	$\delta\Sigma_{rem}$	$\delta\Sigma_{a,1}$	$\delta\Sigma_{a,2}$	$\delta\nu\Sigma_{f,1}$	$\delta\nu\Sigma_{f,2}$
K (cm.°C/pcm)	-0.313	0.818	0.176	-0.821	-0.128

3.3. Derivation of the MTC noise estimators in the 2-D 2-group approximation

In the following, two MTC noise estimators are derived in the 2-D 2-group approximation. The first MTC noise estimator is the one that was used in all the experimental work so far and relies on the local temperature noise, i.e. the neutron noise is measured somewhere in the core, and the temperature noise is measured at the same radial location. The second noise estimator that is worth investigating is the one relying on the core average temperature noise. For both estimators, one further assumes that the reactor behaves in a point-kinetic way at the frequency of interest, therefore the reactivity noise can be approximated by:

$$\delta\rho(\omega) = \frac{1}{G_0(\omega)} \frac{\delta\phi^{pk}(\boldsymbol{r},\omega)}{\phi(\boldsymbol{r})} \tag{67}$$

where $G_0(\omega)$ is the zero-power reactor transfer function, i.e. its open-loop transfer function, and $\delta\phi^{pk}(\boldsymbol{r},\omega)$ is the point-kinetic component of the flux noise[5]. Consequently, the second noise estimator, i.e. the one that was suggested by us recently (see (Pázsit et al, 2000), and (Demazière and Pázsit, 2002)), is expected to be biased only by the deviation

5. In this study, $\delta\phi^{pk}(\boldsymbol{r},\omega)$ and $\phi(\boldsymbol{r})$ represent the contribution of both the fast and thermal groups, whereas it is more likely that the in-core neutron detectors are only sensitive to the thermal flux.

of the reactor response from point-kinetics, whereas the first noise estimator is also biased by the non-homogeneous structure of the temperature noise throughout the core.

The traditional noise estimator, i.e. the one using the local temperature noise, is defined as:

$$H_1^{biased}(\boldsymbol{r}, \omega) = \frac{1}{G_0(\omega)\phi(\boldsymbol{r})} \frac{CPSD_{\delta\phi,\, \delta T_m}(\boldsymbol{r}, \omega)}{APSD_{\delta T_m}(\boldsymbol{r}, \omega)} \tag{68}$$

where the *CPSD* and *APSD* stand for the Cross-Power Spectral Density and the Auto-Power Spectral Density respectively. This noise estimator can be numerically evaluated in the two-group approximation by using the static core simulator, and the neutron noise simulator. One gets:

$$H_1^{biased}(\boldsymbol{r}, \omega) = \frac{1}{G_0(\omega)[\phi_1(\boldsymbol{r}) + \phi_2(\boldsymbol{r})]K} \times \frac{\int [G_{XS \to 1}(\boldsymbol{r}, \boldsymbol{r}', \omega) + G_{XS \to 2}(\boldsymbol{r}, \boldsymbol{r}', \omega)] CPSD_{\delta XS}(\boldsymbol{r}', \boldsymbol{r}, \omega) d\boldsymbol{r}'}{APSD_{\delta XS}(\boldsymbol{r}, \omega)} \tag{69}$$

where $G_{XS \to i}(\boldsymbol{r}, \boldsymbol{r}', \omega)$, $i = 1, 2$ represents the 2-D 2-group discretised Green's function estimated by the neutron noise simulator, in the fast and thermal groups respectively.

The new noise estimator, i.e. the one relying on the core average of the temperature noise, is given by:

$$\tilde{H}_1^{biased}(\boldsymbol{r}, \omega) = \frac{1}{G_0(\omega)\phi(\boldsymbol{r})} \frac{CPSD_{\delta\phi,\, \delta T_m^{ave}}(\boldsymbol{r}, \omega)}{APSD_{\delta T_m^{ave}}(\boldsymbol{r}, \omega)} \tag{70}$$

This noise estimator can also be numerically evaluated in the two-group approximation by using the static core simulator, the adjoint core simulator, and the neutron noise simulator. One gets:

$$\tilde{H}_1^{biased}(\boldsymbol{r}, \omega) = \frac{\int w_{\Delta XS}(\boldsymbol{r}) d\boldsymbol{r}}{G_0(\omega)[\phi_1(\boldsymbol{r}) + \phi_2(\boldsymbol{r})]K} \times \frac{\iint [G_{XS \to 1}(\boldsymbol{r}, \boldsymbol{r}', \omega) + G_{XS \to 2}(\boldsymbol{r}, \boldsymbol{r}', \omega)] CPSD_{\delta XS}(\boldsymbol{r}', \boldsymbol{r}'', \omega) w_{\Delta XS}(\boldsymbol{r}'') d\boldsymbol{r}' d\boldsymbol{r}''}{\iint CPSD_{\delta XS}(\boldsymbol{r}', \boldsymbol{r}'', \omega) w_{\Delta XS}(\boldsymbol{r}') w_{\Delta XS}(\boldsymbol{r}'') d\boldsymbol{r}' d\boldsymbol{r}''} \tag{71}$$

The noise estimators given by Eqs. (69) and (71) have to be spatially discretised in 2-D. Since the static core simulator, the adjoint core simulator, and the neutron noise simulator only give node-averaged values of the static flux, the adjoint flux, and the

neutron noise respectively, the noise estimators can only be approximated since a discretisation that preserves the reaction rates requires the spatially-dependent static flux, adjoint flux, and neutron noise within each node.

One therefore gets for the $H_1^{biased}(\boldsymbol{r}, \omega)$ noise estimator:

$$H_{1,I,J}^{biased}(\omega) = \frac{1}{G_0(\omega)[\phi_{1,I,J} + \phi_{2,I,J}]K} \times \frac{\sum_{I',J'} [G_{XS \to 1,(I',J') \to (I,J)}(\omega) + G_{XS \to 2,(I',J') \to (I,J)}(\omega)] CPSD_{\delta XS,(I',J'),(I,J)}(\omega)\Delta x \Delta y}{APSD_{\delta XS,I,J}(\omega)} \tag{72}$$

The summation over (I', J') can be avoided since the neutron noise simulator is able to calculate the flux noise induced by a spatially distributed noise source. The following methodology can therefore be applied:

- For each (I, J) pair, one calculates the neutron noise $\delta\phi_{1,I,J}(\omega)$ and $\delta\phi_{2,I,J}(\omega)$ induced by the spatially distributed noise source $CPSD_{\delta XS,(I',J'),(I,J)}$;
- The discretised $H_1^{biased}(\boldsymbol{r}, \omega)$ noise estimator is thus given by:

$$H_{1,I,J}^{biased}(\omega) = \frac{1}{G_0(\omega)[\phi_{1,I,J} + \phi_{2,I,J}]K} \times \frac{\delta\phi_{1,I,J}(\omega) + \delta\phi_{2,I,J}(\omega)}{APSD_{\delta XS,I,J}(\omega)} \tag{73}$$

For the $\tilde{H}_1^{biased}(\boldsymbol{r}, \omega)$ noise estimator now, one has:

$$\tilde{H}_{1,I,J}^{biased}(\omega) = \frac{\sum_{I',J'} w_{\Delta XS,I',J'}}{G_0(\omega)[\phi_{1,I,J} + \phi_{2,I,J}]K} \times \frac{\sum_{I',J'} [G_{XS \to 1,(I',J') \to (I,J)}(\omega) + G_{XS \to 2,(I',J') \to (I,J)}(\omega)] \sum_{I'',J''} CPSD_{\delta XS,(I',J'),(I'',J'')}(\omega) w_{\Delta XS,I'',J''} \Delta x^2 \Delta y^2}{\sum_{I',J'} \sum_{I'',J''} CPSD_{\delta XS,(I',J'),(I'',J'')}(\omega) w_{\Delta XS,I',J'} w_{\Delta XS,I'',J''} d\boldsymbol{r}' d\boldsymbol{r}''} \tag{74}$$

As before, the summation over (I', J') can be avoided in the numerator of Eq. (74) since the neutron noise simulator is able to calculate the flux noise induced by a spatially distributed noise source. The following methodology can therefore be applied:

- For each (I, J) pair, one calculates the neutron noise $\delta\phi_{1,I,J}(\omega)$ and $\delta\phi_{2,I,J}(\omega)$ induced by the spatially distributed noise source $\sum_{I'',J''} CPSD_{\delta XS,(I',J'),(I'',J'')}(\omega) w_{\Delta XS,I'',J''} \Delta x \Delta y$;
- The discretised $\tilde{H}_1^{biased}(\boldsymbol{r}, \omega)$ noise estimator is thus given by:

$$\tilde{H}_{1,I,J}^{biased}(\omega) = \frac{\sum_{I',J'} w_{\Delta XS,I',J'}}{G_0(\omega)[\phi_{1,I,J}+\phi_{2,I,J}]K} \tag{75}$$

$$\times \frac{\delta\phi_{1,I,J}(\omega)+\delta\phi_{2,I,J}(\omega)}{\sum_{I',J'}\sum_{I'',J''} CPSD_{\delta XS,(I',J'),(I'',J'')}(\omega) w_{\Delta XS,I',J'} w_{\Delta XS,I'',J''} d\boldsymbol{r}' d\boldsymbol{r}''}$$

The static core simulator, the adjoint core simulator, the neutron noise simulator, the calculation of the coefficient K depending on the noise source type, and the derivation of the MTC noise estimators can be checked by running a test case. Namely, one assumes that the temperature noise is spatially homogeneous throughout the core. In such a case, the reactor behaves in a point-kinetic way (Demazière and Pázsit, 2002), and the local temperature noise is identical to the core average temperature noise. Consequently, the $H_1^{biased}(\boldsymbol{r},\omega)$ noise estimator should provide the correct MTC value. As can be seen in Figs. 7 - 11, the correct MTC value is given throughout the core. The $\tilde{H}_1^{biased}(\boldsymbol{r},\omega)$ noise estimator is obviously identical to the $H_1^{biased}(\boldsymbol{r},\omega)$ noise estimator in such a case (homogeneous temperature noise in the core).

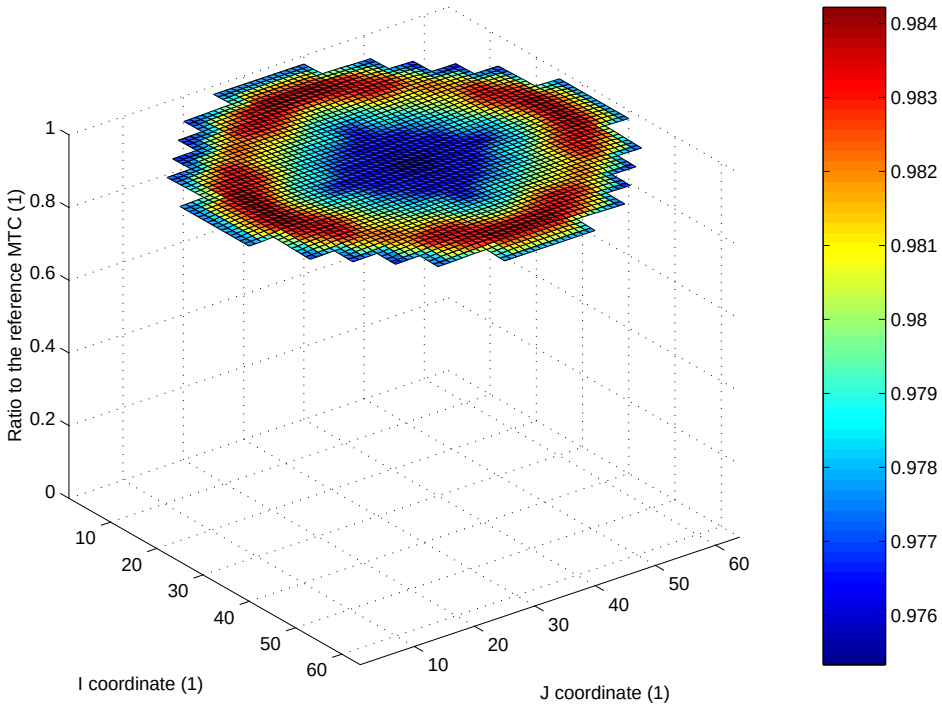

Figure 7: MTC noise estimation in case of a spatially homogeneous temperature noise proportional to the macroscopic removal cross-section noise

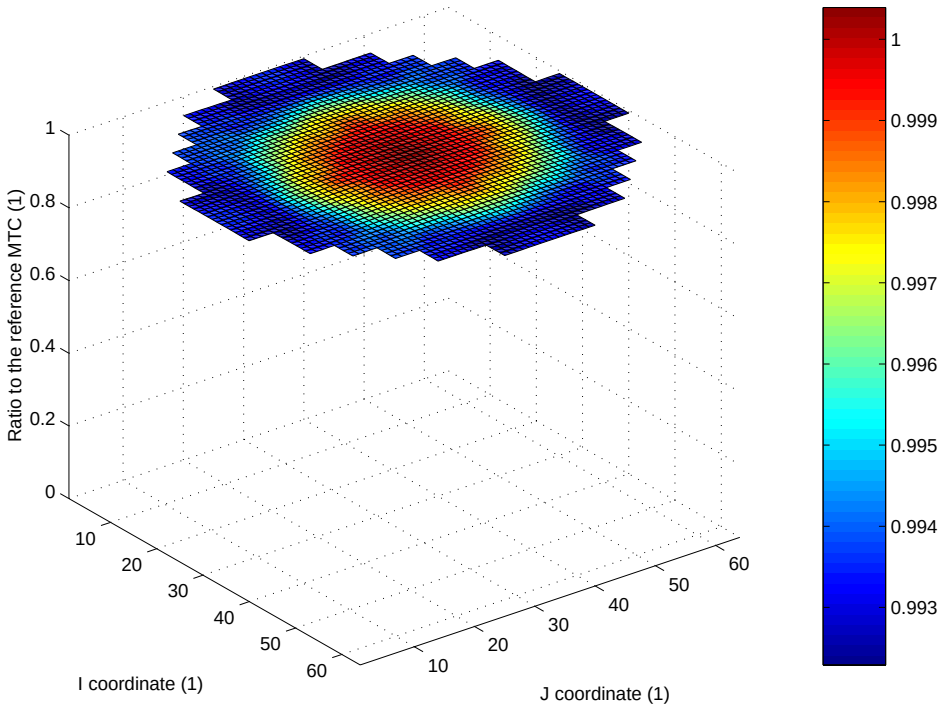

Figure 8: MTC noise estimation in case of a spatially homogeneous temperature noise proportional to the macroscopic fast absorption cross-section noise

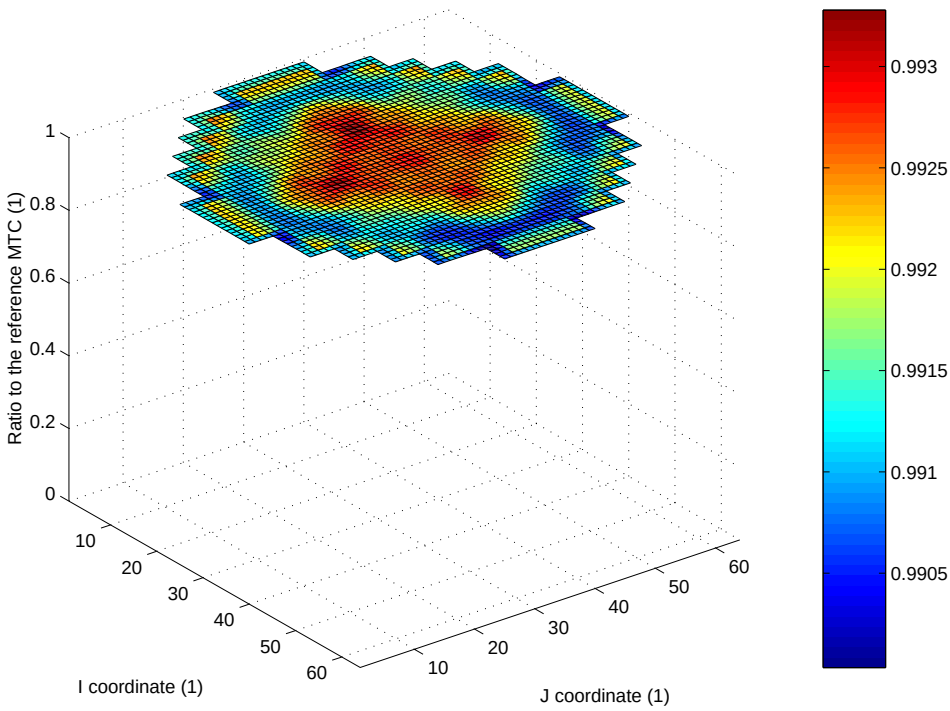

Figure 9: MTC noise estimation in case of a spatially homogeneous temperature noise proportional to the macroscopic thermal absorption cross-section noise

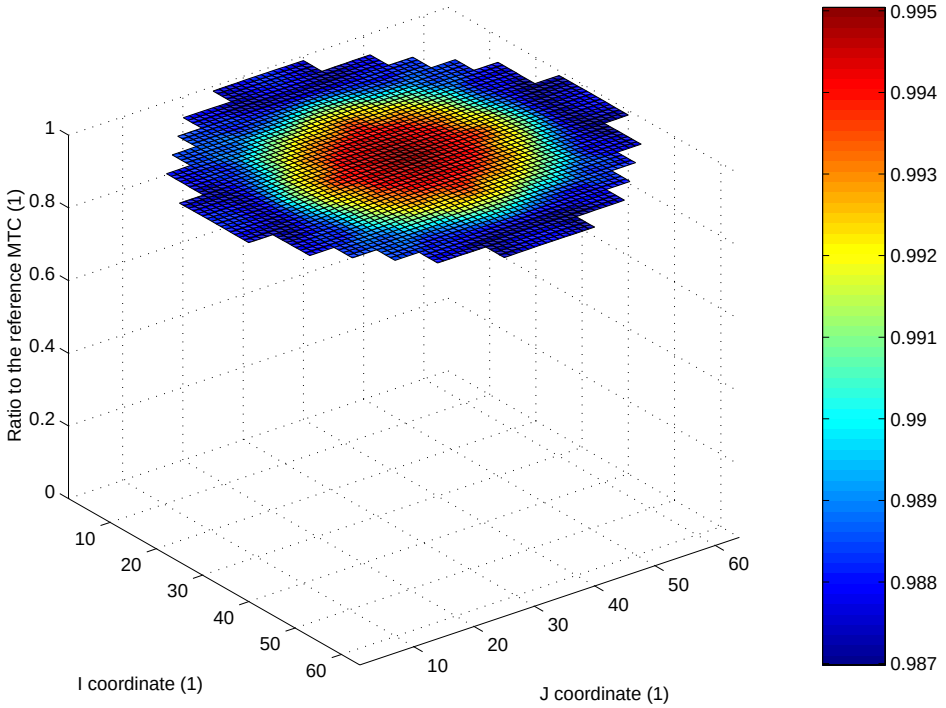

Figure 10: MTC noise estimation in case of a spatially homogeneous temperature noise proportional to the macroscopic fast fission cross-section noise

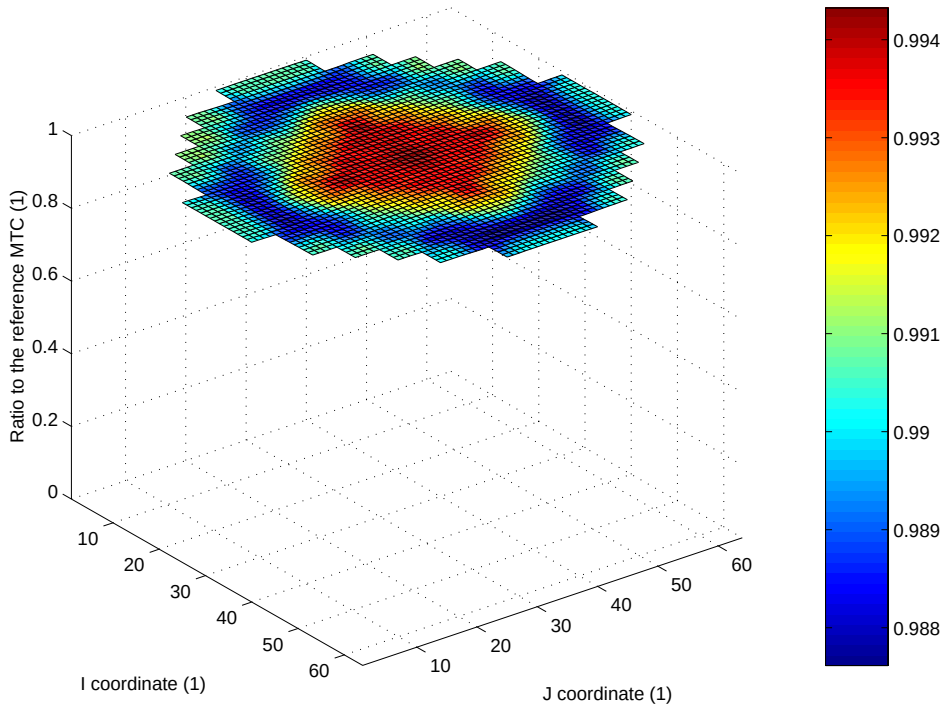

Figure 11: MTC noise estimation in case of a spatially homogeneous temperature noise proportional to the thermal fission cross-section noise

4. Results

In the following, the results of the theoretical MTC noise investigations are presented. As mentioned previously, all the calculations were performed at the frequency of 1 Hz. Furthermore, only one given core burnup was considered, i.e. 8.767 GWd/tHM. The fact that the usual MTC noise estimator, i.e. $H_1^{biased}(\boldsymbol{r}, \omega)$, underestimates the actual MTC value by a constant factor throughout the fuel cycle will be therefore investigated at a later stage.

4.1. Specification of the noise source

In this study, only the macroscopic removal cross-section noise source is studied, since the reactivity effect induced by a change in the moderator temperature on the removal cross-section is the most significant one (see Table 4).

As presented in (Demazière and Pázsit, 2002), the noise source is defined directly through its spatial statistical properties as:

$$CPSD_{\delta\Sigma_{rem}}(\boldsymbol{r}, \boldsymbol{r}', \omega) = \sigma^2(\hat{r}) e^{-\frac{|\boldsymbol{r}-\boldsymbol{r}'|}{l}} \tag{76}$$

with

$$\hat{r} \equiv \frac{|\boldsymbol{r} + \boldsymbol{r}'|}{2} \tag{77}$$

and where $\sigma^2(\hat{r})$ represents the noise source strength, i.e. its *APSD*. Different $\sigma^2(\hat{r})$ functions are planned to be investigated in the future. In this study, only one type of shape function is investigated. Namely, one has:

$$\sigma(\hat{r}) = \frac{1}{1 - \left(\frac{\hat{r}}{R + \delta R}\right)^2} \tag{78}$$

where R is the core radius and $\delta R = R/5$. This shape function corresponds to some experimental evidence that the temperature noise is larger close to the core boundary than at the core centre (Karlsson, 2000). In this model, l is called the correlation length of the temperature fluctuations and is supposed to be space independent. The correlation length indicates roughly the maximum distance between two points that can be considered as having a coherent behaviour. For greater distances, their behaviour can be assumed to be completely uncorrelated. Several correlation lengths are investigated in this study: $l = 15$ cm, $l = 150$ cm, and $l = 300$ cm.

Eq. (76) has to be used as a noise source for the neutron noise simulator. Therefore, this noise source needs also to be spatially discretised in 2-D. A rigorous discretisation would be to calculate the following quantities:

$$CPSD_{\delta\Sigma_{rem},(I,J),(I',J')}(\omega) = \frac{1}{\Delta x^2 \Delta y^2} \int_{(I,J)} \int_{(I',J')} \sigma^2\left(\frac{|\boldsymbol{r}+\boldsymbol{r}'|}{2}\right) e^{-\frac{|\boldsymbol{r}-\boldsymbol{r}'|}{l}} d\boldsymbol{r}\, d\boldsymbol{r}' \qquad (79)$$

This discretised *CPSD* function is relatively complex to evaluate, since in 2-D this corresponds to a quadruple spatial integral. Therefore, a more simple way of discretizing the *CPSD* function was adopted, namely the *CPSD* function was discretised by simply choosing the value of the function in the middle of each node. The corresponding discretised *APSD* function can be seen in Fig. 12.

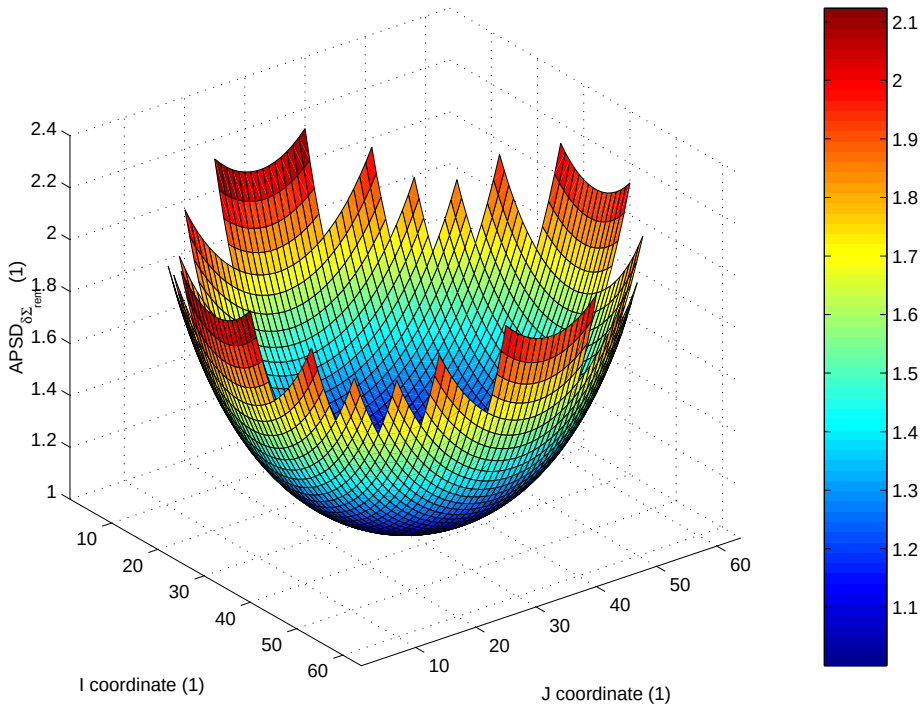

Figure 12: Discretised APSD function

4.2. Calculated MTC noise estimators

A comparison of the traditional $H_1^{biased}(\boldsymbol{r},\omega)$ MTC noise estimator and the new $\tilde{H}_1^{biased}(\boldsymbol{r},\omega)$ MTC noise estimator to the true MTC is plotted for a correlation length of $l = 15$ cm in Fig. 13, for a correlation length of $l = 150$ cm in Fig. 14, and for a correlation length of $l = 300$ cm in Fig. 15.

As can be seen in these Figures, the new $\tilde{H}_1^{biased}(\boldsymbol{r},\omega)$ MTC noise estimator always correctly estimates the actual value of the MTC, whatever the correlation length of the temperature noise is and whatever the location of the measurement of the neutron noise is. Since this noise estimator still relies on a point-kinetic behaviour of the reactor, this suggests that the deviation of the reactor response from point-kinetics is negligible with respect to the MTC determination. Consequently, measuring the total flux noise instead of only its point-kinetic component does not seem to affect significantly the

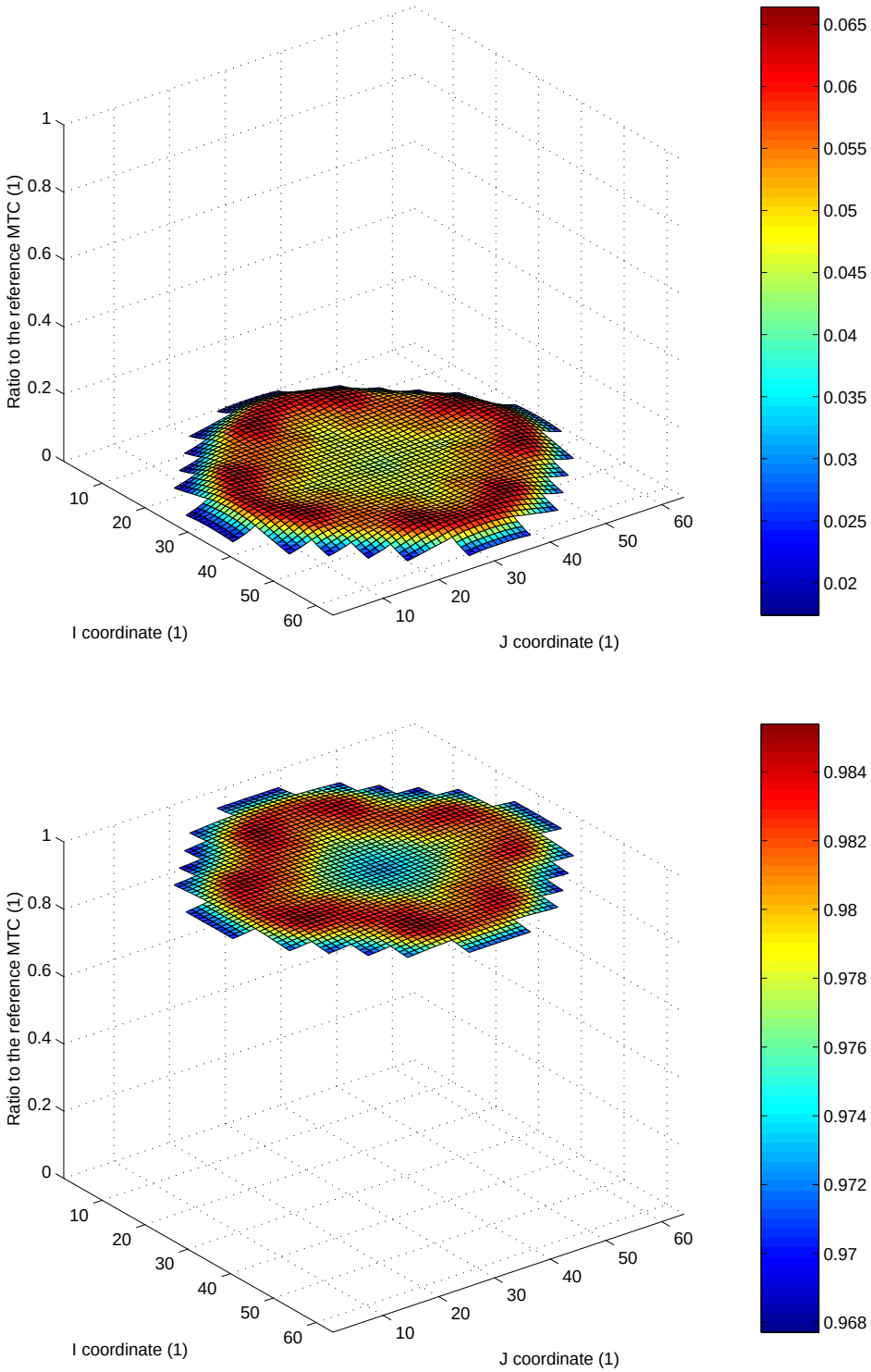

Figure 13: Comparison between $H_1^{biased}(\boldsymbol{r}, \omega)$ *and the actual MTC value (upper figure), and between* $\tilde{H}_1^{biased}(\boldsymbol{r}, \omega)$ *and the actual MTC value (lower figure), for a correlation length of* $l = 15$ cm

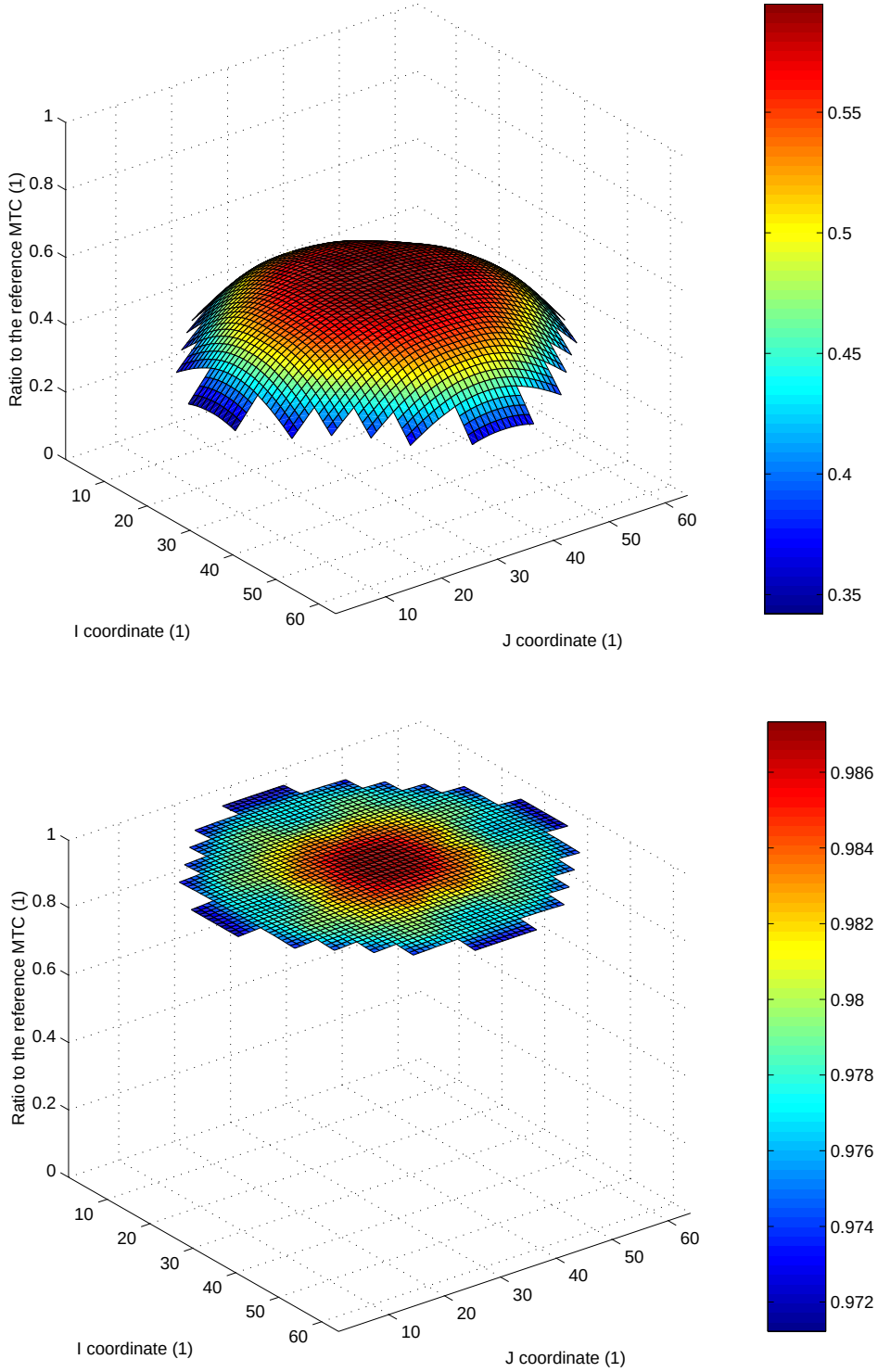

Figure 14: Comparison between $H_1^{biased}(\boldsymbol{r}, \omega)$ *and the actual MTC value (upper figure), and between* $\tilde{H}_1^{biased}(\boldsymbol{r}, \omega)$ *and the actual MTC value (lower figure), for a correlation length of* $l = 150$ cm

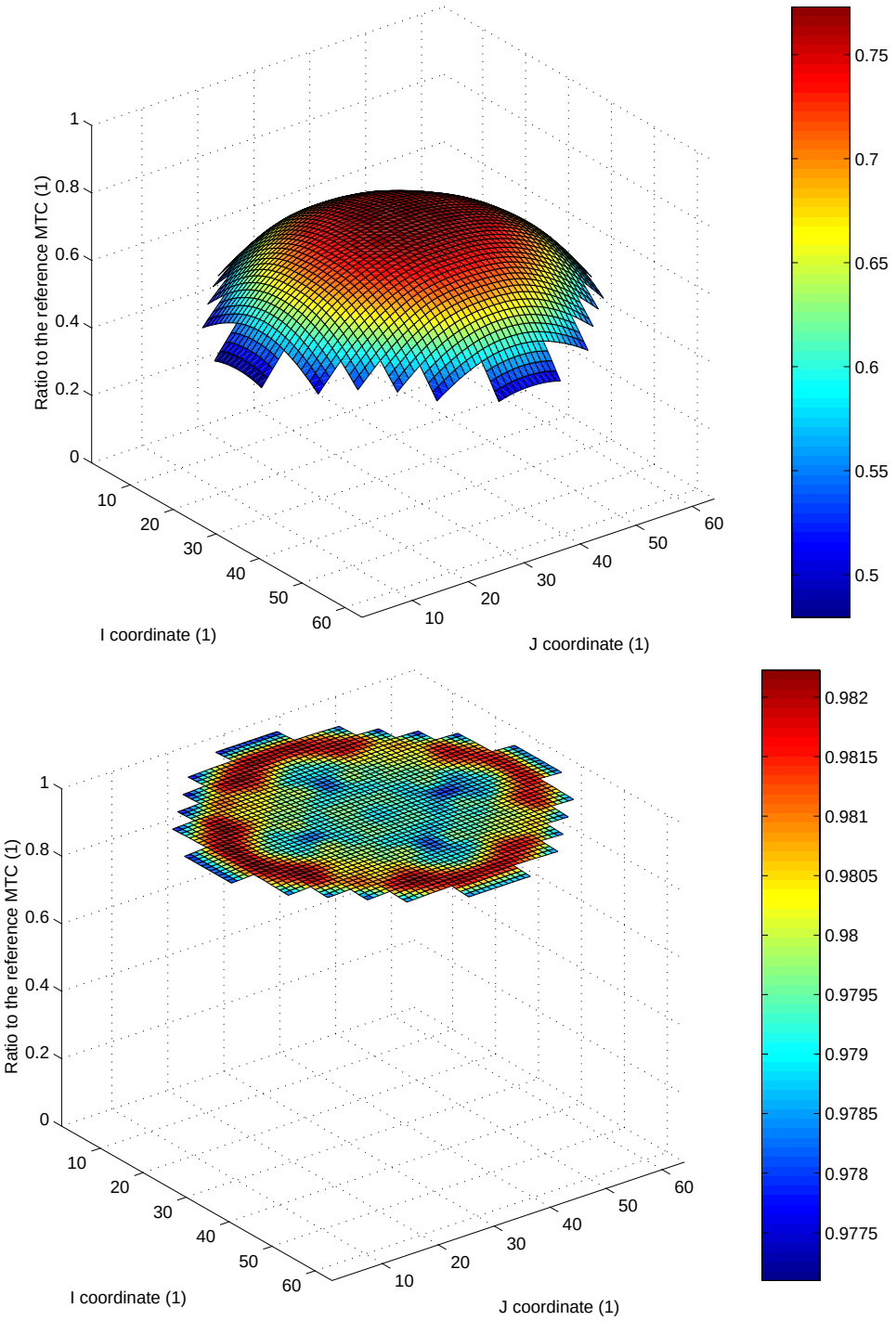

Figure 15: Comparison between $H_1^{biased}(\boldsymbol{r}, \omega)$ *and the actual MTC value (upper figure), and between* $\tilde{H}_1^{biased}(\boldsymbol{r}, \omega)$ *and the actual MTC value (lower figure), for a correlation length of* $l = 300$ cm

accuracy of the noise analysis technique (as can be seen on the Figures, the discrepancy due to the fact that the reactor does not behave perfectly in a point-kinetic manner is less than 4%).

In contrast to the new MTC noise estimator, the traditional $H_1^{biased}(\boldsymbol{r}, \omega)$ noise estimator is systematically biased low compared to the actual MTC value. The smaller the correlation length of the temperature noise is, the bigger the discrepancy is. This traditional MTC noise estimator is also strongly space-dependent. Compared to the previous 1-D study in a homogeneous reactor, the underestimation seems to be larger in 2-D than in 1-D for the same correlation length. Furthermore, the discrepancy in the 2-D case seems to be also more homogeneous than in the 1-D case. If one tries to relate these theoretical investigations to the experimental MTC noise studies performed so far, it seems that in the centre of the core a realistic correlation length seems to be around 100 - 150 cm in the 2-D system, because with this correlation length the underestimation of the $H_1^{biased}(\boldsymbol{r}, \omega)$ estimator is about a factor five, which corresponds to the experimental results so far. The same underestimation in the 1-D case was obtained with a correlation length of about 15 cm.

5. Conclusions

In this study, the effect of a non-homogeneous distribution of the moderator temperature noise on the MTC estimation by noise analysis was investigated. All the models relied on the 2-group diffusion approximation, and realistic data corresponding to a commercial nuclear reactor were axially condensed in 2-D.

It was found that the main reason why the traditional MTC noise estimator systematically underestimates the actual value of the MTC lies with the fact that the temperature noise might be radially heterogeneous, whereas this traditional MTC estimator only uses the temperature noise at the same radial location as the neutron noise. Another noise estimator (already proposed in (Pázsit et al, 2000)) was tested and was proven to always give the correct MTC value within an accuracy of 4% of the design-predicted MTC value. This slight discrepancy results from the deviation of the reactor response from point-kinetics, an approximation on which this new MTC noise estimator still relies. The main difference between the new and traditional MTC noise estimators is that the new one takes the heterogeneous structure of the temperature noise into account.

As a matter of fact, this estimator is based on the core average temperature noise that has first to be estimated. This estimation relies on the possibility of measuring the coolant temperature noise inside the core, and then on calculating the average by using a proper weighting function. Several weighting functions are possible depending on the type of noise source that is assumed to be the most sensitive to the coolant temperature noise.

Such weighting functions are planned to be tested in the near future since a noise measurement was recently performed in Ringhals-2, measurement in which Gamma-Thermometers (GTs) were used together with a couple of in-core neutron detectors and a core-exit thermocouple. It was proven that GTs are actually working as ordinary thermocouples in the frequency range of interest for the MTC investigation by noise

analysis. Therefore, these GTs offer a unique opportunity to test this new MTC noise estimator, and to compare it to the traditional one. If the heterogeneous structure of the temperature noise is actually responsible for the underestimation of the MTC noise estimation via the traditional noise estimator, then the new one should give the correct MTC value.

6. References

ANSI, *Calculation and measurement of the moderator temperature coefficient of reactivity for water moderated power reactors, an American National Standard*, American Nuclear Society, ANSI/ANS-19.11-1997, 1997

Bell, G.I., Glasstone, S., *Nuclear Reactor Theory*, Van Nostrand Reinhold Company, New York, 1970

Demazière, C., Arzhanov, V., Pázsit, I., *Final Report on the Research Project Ringhals Diagnostics and Monitoring, Stage 5*, CTH-RF-156/RR7, Chalmers University of Technology, Göteborg, Sweden, 2000

Demazière, C., Pázsit, I., Pór, G., *Estimation of the moderator temperature coefficient (Analysis of an MTC measurement using boron dilution method)*, In: Proceedings of NPIC&HMIT 2000, Embedded Topical Meeting #1: International Topical Meeting on Nuclear Plant Instrumentation, Controls, and Human-Machine Interface Technologies, November 13-16, 2000, Washington, DC, USA

Demazière, C., *Development of a non-intrusive method for the determination of the moderator temperature coefficient of reactivity (MTC)*, CTH-RF-157, Chalmers University of Technology, Göteborg, Sweden, 2000

Demazière, C., Pázsit, I., *Theoretical investigation of the MTC noise estimate in 1-D homogeneous systems*, Annals of Nuclear Energy, **29**, pp. 75-100, 2002

Karlsson, J. K.-H., GSE Power Systems AB, Nyköping, Sweden, personal communication, 2000

Nakamura, S., *Computational Methods in Engineering and Science With Applications to Fluid Dynamics and Nuclear Systems*, Wiley Interscience, New York, 1977

Pázsit, I., Demazière, C., Avdic, S., Dahl, B., *Research and Development Program in Reactor Diagnostics and Monitoring with Neutron Noise Methods, Stage 6, Final report*, SKI report 00:28, Swedish Nuclear Power Inspectorate, Stockholm, Sweden, 2000

Pázsit, I., Demazière, C., Arzhanov, V., Garis, N. S., *Research and Development Program in Reactor Diagnostics and Monitoring with Neutron Noise Methods, Stage 7, Final report,* SKI report 01:27, Swedish Nuclear Power Inspectorate, Stockholm, Sweden, 2001

Umbarger, J. A., DiGiovine, A. S., *SIMULATE-3, Advanced Three-Dimensional Two-Group Reactor Analysis Code, User's Manual*, Studsvik Report, Studsvik of America, 1992

7. Nomenclature

APSD	Auto-Power Spectral Density
BOC	Beginning Of Cycle
CPSD	Cross-Power Spectral Density
EOC	End Of Cycle
GT	Gamma-Thermometer
HZP	Hot Zero Power
MTC	Moderator Temperature Coefficient
MOX	Mixed Oxide
PWR	Pressurized Water Reactor